EVALUATION OF TARGETING SCHEMES FOR COMPLEMENT-MODULATING, STRAIN-SELECTIVE ANTIMICROBIAL MICROPARTICLES

A Thesis
Presented to
The Academic Faculty

By

Michael Bellavia

In Partial Fulfillment of the Requirements for the Degree
Master of Science in the
Wallace H. Coulter Department of Biomedical Engineering

Georgia Institute of Technology and Emory University
May 2018

EVALUATION OF TARGETING SCHEMES FOR COMPLEMENT-MODULATING, STRAIN-SELECTIVE ANTIMICROBIAL MICROPARTICLES

Approved by:

Todd Sulchek PhD, Advisor
School of Mechanical Engineering
Georgia Institute of Technology

Julia E. Babensee, PhD
Department of Biomedical Engineering
Georgia Institute of Technology

Sean R. Stowell, M.D./PhD
Department of Pathology and Laboratory Medicine
Emory University School of Medicine

Date Approved: April 19, 2018

To all who supported me

ACKNOWLEDGEMENTS

Foremost I would like to thank Dr. Todd Sulchek for his willingness to support me in this endeavor. I did not come to him under the best of circumstances, but he believed in me regardless. Even with several pivots and my decision to continue my studies elsewhere, he was always willing to guide me.

The friendship and support I received from my colleagues in the Sulchek BioMEMS and Biomechanics Laboratory were pivotal in completing this project. In particular, I wish to recognize Kathryn Murray, Betsy Campbell, and Katily Ramirez for their advice and assistance on technical matters. Brandon Holt was instrumental both as a mentor and later for his assistance. I also want to thank my undergraduate students Winston Wu, Renee Puvvada, and Krina Patel for their efforts, even in my absence.

I would like to thank Ashley Frantellizzi for her unwavering support and reassurance. She has always inspired me to continue when my confidence or motivation falters.

My parents Kathryn Jivoff and Charles Bellavia, as well as other members of my family, provided encouragement that has sustained me throughout my graduate career.

Lastly, I would like to thank all of those who have provided friendship and support during my time at Georgia Tech.

TABLE OF CONTENTS

LIST OF FIGURES

LIST OF ABBREVIATIONS

APC	Allophycocyanin
BSA	Bovine serum albumin
EDC	1-Ethyl-3(dimethylaminopropyl)carbodiimide
Dnk	Donkey, referring to origin of particular IgG
Fc	Fragment crystallizable region (of an antibody)
x G	Centrifugal force (times gravity)
Gt	Goat, referring to origin of particular IgG
HI	Heat-inactivated
IgG	Immunoglobulin G
LPS	Lipopolysaccharide
MBL	Mannose-binding lectin
Ms	Mouse, referring to origin of particular IgG
MUT	Mixed untargeted particles
MT	Mixed targeted particles
NH_2	An amine group
PAMP	Pathogen-associated molecular pattern
PBS	Phosphate-buffered saline
PEG	Polyethylene glycol
Rb	Rabbit, referring to origin of particular IgG
SA	Streptavidin
TCC	Terminal complement complex
UT	Untargeted particles

SUMMARY

Here we present bifunctional microparticles that bind *Escherichia coli* (*E. coli*) bacteria via a cell membrane constituent while also activating the classical complement pathway. Carboxylated polystyrene microparticles 1 μm in diameter were functionalized through several means with nonspecific polyclonal IgG and/or a monoclonal *E. coli*-binding antibody to compare different targeting schemes to localize complement to a particular bacterial strain. The complement-prompting polyclonal antibody was either adsorbed to saturate the particle nonspecifically (Untargeted, UT), adsorbed nonspecifically at half-saturation in combination with the targeting antibody (Mixed Untargeted, MUT), or interspersed amongst crosslinker-monoclonal antibody pairs formed such that the antibody F_{ab} regions project outward (MT, Mixed Targeted). Cytotoxicity of each particle type to its cognate, either complement-sensitive non-pathogenic mutant *E. coli* J5 and wild-type pathogenic *E. coli* O157:H7 was evaluated, as was targeting affinity for anti-J5 particles and J5 bacteria. Although no type provided clinically-relevant cytotoxicity, notably the MUT particles were somewhat effective against the virulent and otherwise complement-resistant O157. Orienting the targeting moiety with the MT provided no benefit against either strain, and binding frequencies were attenuated relative to the MUT for J5 bacteria. Complement-sensitive J5 was most vulnerable to UT particles. In most cases, there was a correlation between increased cytotoxicity and the extent of IgG coverage, but this effect was generally not pronounced. Additional modifications to the MUT platform to more potently stimulate complement activation and a new base material for biocompatibility could enable its use as a sensitizer to be paired with antibiotics for systemic diseases such as sepsis or candidiasis.

CHAPTER 1: INTRODUCTION

1.1 Antimicrobial Resistance and Conventional Antibiotics

Multidrug antimicrobial resistance (AMR) in bacteria is a universal, growing healthcare problem – methicillin-resistant *Staphylococcus aureus* (MRSA) and *Clostridium difficile* are well-known, but certain Gram-negative strains, such as *Klebsiella pneumoniae,* may resist almost all known antibiotics [1]. Approximately 2 million new cases of AMR emerge in the United States each year, contributing to more than 20,000 deaths, many of which are preventable [2, 3]. To counter otherwise lethal selective pressure, bacteria will continuously develop means to evade antibiotics or reduce their effectiveness – more than 70% of disease-causing bacteria are estimated to resist at least one antibiotic in common use [4]. By 2050, the WHO projects AMR to be responsible for more annual mortalities than cancer and diabetes [5] (**Figure 1.1 A**). This issue is exacerbated further by a reduction of novel antibiotics coming to market; the number of antibiotics receiving FDA approval has fallen 90% during the past three decades [6]. Of those currently in the clinic, few are effective against Gram-negative strains that are often extensively drug-resistant, namely the *Enterobacteriaceae* (which include *Escherichia coli* and *Klebsiella*) and *Pseudomonas aeruginosa* [7]. The pharmaceutical pipeline is also deficient, as industry has favored antibiotic development against methicillin-resistant *Staphylococcus aureus*, given the larger market scope and slower acquisition of resistance (**Figure 1.1 B**). Investment in antibiotic development is also less appealing given recently revised FDA stipulations to study designs required for regulatory approval, greatly increasing cost [8].

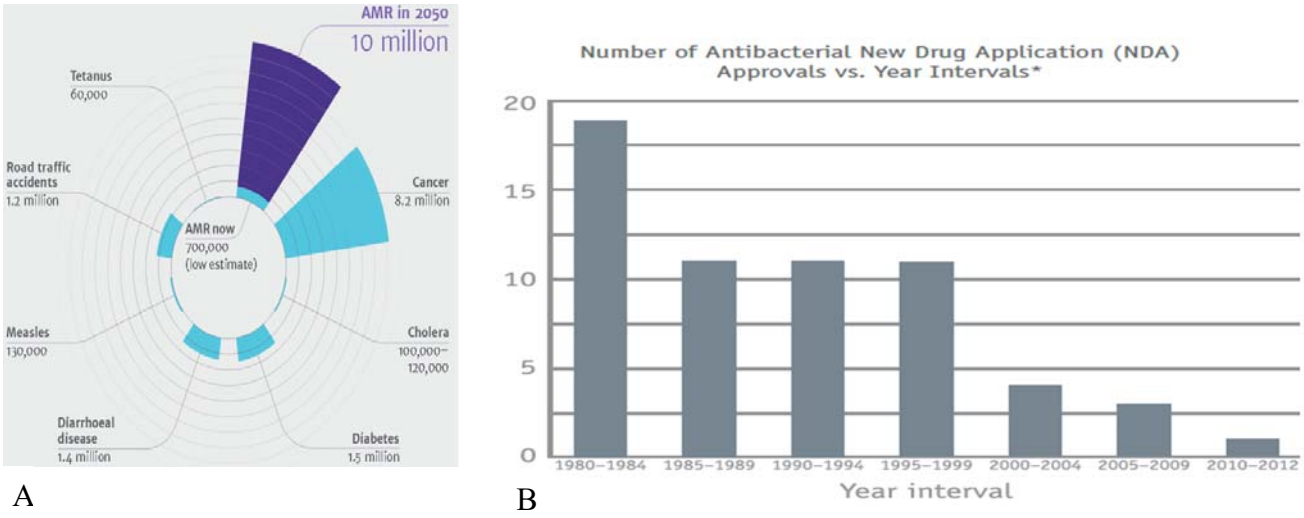

Figure 1.1: Despite a growing public health concern, antibiotic development has not kept pace. (A) By 2050, deaths attributed to drug resistance in bacteria globally are estimated to supersede those of more notorious public health issues. Figure adapted from the Review on Antimicrobial Resistance**.** *Antimicrobial Resistance: Tackling a Crisis for the Health and Wealth of Nations.* 2014 [9]. (B) Novel antibiotic development has fallen precipitously over the past several decades, likely due to fewer economic incentives. Figure from CDC. *Antibiotic Resistance Threats.* 2013 [3].

As antibiotics in clinical use are non-specific, susceptible commensal bacteria inhabiting the epithelial surfaces of the body (the airways, mucosa, skin, and digestive tract) are killed, facilitating colonization by resistant pathogenic bacteria. Not only do commensals compete with pathogens for nutrients, but they may release antimicrobials such as bacteriocidins or prompt immunostimulatory pathways, such as triggering Paneth cells in proximity to release C-type lectins and defensins [10, 11]. Some of these agents show considerable promise as novel antibiotics, and are only now being elucidated [12]. In addition, accumulating evidence implicates antibiotic disruption of commensal populations in chronic inflammatory bowel diseases [13, 14], as well as diabetes [15, 16], particularly if given in early life.

1.2 The Complement System

The complement system is an integral component of the innate immune response and refers to a group of 30+ interacting proteins that recognize conserved molecular signatures on

pathogens, initiating their opsonization and lysis [17-19]. The pathway bridges humoral and adaptive immunity, as complement mediators both recruit phagocytes and initiate adaptive immune responses [18, 20, 21]. The tail of each immunoglobulin class, the crystallizable fragment (Fc), is essential in immune priming following pathogen opsonization as it allows for activation of the classical complement pathway, culminating in lysis, but also recognition by neutrophils and macrophages [22-25].

The classical or antibody-mediated pathway (**Figure 1.2**) is activated robustly following the binding of the pattern recognition molecule C1q to proximal Fc regions of multiple IgG antibodies or a single IgM antibody [26, 27]. C1q also recognizes and binds bacteria via pentraxins, a class of plasma proteins that detect foreign and modified self-antigens [28]. The essential pentraxins of human plasma include serum amyloid P (SAP), pentraxin 3, and C-reactive protein [28]. C1q can also directly bind to carbohydrate constituents of pathogen surfaces to initiate the classical pathway [29, 30]. Bound C1q then interacts in series with proteases C1r and C1s. The now activated C1s cleaves C4 into C4a and C4b; a reactive thioester on C4b is exposed such that C4b opsonizes surfaces in proximity to the point of activation. C1s cleaves C2 bound to this C4b, forming C2a and C2b. C2b is critical in that it forms the C3 convertase with C4a. The C3 convertase rapidly cleaves C3 to C3a and C3b. The alternative and lectin-mediated pathways, though initiated via different mediators, merge at the complement opsonin C3b. Concurrent C3b amplification occurs due to alternative pathway activation, as factor B binds surface-bound C3b, forming the alternative pathway C3 convertase (C3bBb) in a compounding loop. C3b serves as the effector of the cytotoxic function of both pathways, as increased C3b binding transitions the main substrate of the convertases from C3 to C5 (C5 convertase: C4b2a3b). A product of C5 cleavage, C5b, forms part of the terminal complement

complex (TCC) or the membrane attack complex (sC5b-C9). TCC forms a pore in the pathogen membrane, resulting in lysis [31]. Anaphylatoxins such as C3a and C5a formed during the cascade trigger the inflammatory response and act as phagocyte chemoattractants [32].

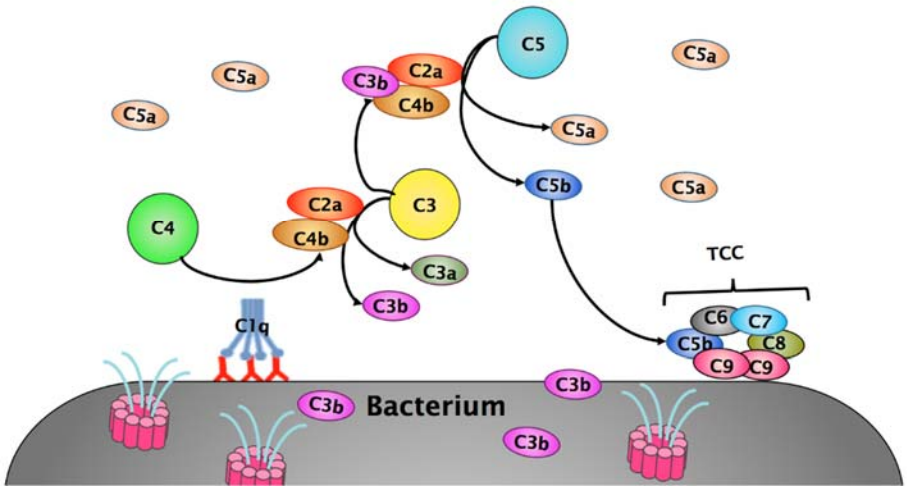

Figure 1.2: A simplified depiction of the classical or antibody-mediated pathway of complement activation. The pathway is initiated by the binding of C1q to antibodies that recognize pathogen-associated molecular patterns (PAMPs) on the bacterium surface. A proteolytic cascade follows, in which the classical C3 convertase (C4b2b) is formed, resulting in C3 cleavage and C3b deposition, in addition to analyphlatoxin C3a/4a generation to spur phagocyte influx and downstream inflammatory responses. From these split products the classical C5 convertase forms (C4b2a3b), and from the cleavage of C5, C5b joins with C6-C9 to form the terminal complement complex (TCC). TCC forms a pore in the membrane, causing lysis. C5a, the other split product of C5, like C3a, is a potent stimulator of further proinflammatory signaling and phagocyte chemotaxis. Figure from [33].

The alternative and lectin pathways, although not explored in this work, function in synergy with the classical complement pathway to destroy pathogens and ensure homeostasis. The alternative pathway serves as sentinel to monitor pathogen entry, as it is constitutively active, with baseline activity via the spontaneous hydrolysis of the thioester of C3 [17, 18]. This bioactive C3 can then be modified to form the alternative C3 convertase, as described above. The lectin pathway is analogous to the classical pathway, in that mannose-binding lectin (MBL) or ficolins recognize and bind to sugar groups of a particular orientation on pathogen surfaces, namely glucose and mannose. Once activated by mannose-associated serine proteases, this

complex cleaves C4 and C2, as does the C1 proenzyme complex. The classical pathway C3 convertase is then formed. With regard to bacterial pathogens, the lectin pathway is essential in countering clinically-relevant Gram-positive bacteria, including *Streptococcus pneumoniae* [34] and *Staphylococcus aureus* [35] though also involved in the response to Gram-negative *Pseudomonas aeruginosa* [35].

1.3 Particle Platforms for Complement Activation

By convention, microparticle and nanoparticle formulations intended for therapeutic or diagnostic use are designed to limit opsonization by serum proteins and complement, as this reduces phagocyte uptake and subsequent immune responses. Perhaps the most extensively utilized approach is to engineer the surface chemistry, usually by integrating poly(ethylene glycol) (PEG) or particular zwitterionic polymers to form a hydration shell around the particle and thereby sterically hinder protein adsorption [36, 37]. However, as the role of complement in adaptive immunity has been clarified, there has been increasing interest in using particle platforms to induce complement activation and modulate sought elements of this response. The complement protein C3 and its split products C3b and iC3b (inactivated C3b opsonin) are intriguing effectors to target, as C3 and antigen-bound C3b has been demonstrated to boost inflammatory T cell activity [20, 38], whereas iC3b binding to dendritic cells may promote tolerance [39, 40]. This induction of tolerance likely contributes to tumor evasion of immune surveillance.

Complement-stimulating capability in the context of tuning adaptive immunity has been most extensively studied regarding material surface chemistry. These particles are intended almost exclusively as vaccines. Reddy and colleagues introduced complement-activating

poly(propylene sulfide) nanoparticles that preferentially accumulated in the lymph nodes and prompted specific, complement-dependent immunity *in vivo* [41]. Given the high density of hydroxyl groups on the particle surface due to Pluronic stabilization, it was purported that they readily bound C3b and initiated activation via the alternative pathway. Thomas *et al.* improved upon this further, providing better control of C3b deposition on the particles by increasing the negative surface charge and nucleophile abundance with the addition or substitution of/with carboxyl-terminated Pluronic [42]. Others have utilized complement-modulating microparticles in tandem with vaccines, and found that those cross-linked with C3b-binding moieties provide higher antigen-specific antibody titers and increased inflammatory cytokine production upon restimulation *ex vivo* [43]. In addition to materials chemistry, it appears that complement-modulating particle morphologies that delay lymphatic drainage, extending the duration of complement signaling in antigen presentation, best augment immune responses [44].

Although there is extensive understanding of the influence of Fc valency and orientation in the regulation of complement activation *in vitro* and its influence in the downstream immune response [45-47], there is little work comparatively with Fc-coated platforms. Of this, much of the work related to Fc-coated microparticles in immunomodulation concerns how they may be employed to spur macrophage phagocytosis and cytokine release [48-51]. As we have previously demonstrated, Fc-coated microparticles can be designed to substantially modulate the complement cascade by tuning Fc valency and sterics as a result of Fc abundance on the particle surface [50, 52]. Interestingly, we have shown that by coating microparticles with the antigen recognized by the initiating IgG such that the IgG binds in a uniform orientation, there is a immunosuppressive response *in vitro* [33]. But when the antigen coating is absent and the IgG binds randomly, robust complement activation is better localized into the surrounding milieu,

increasing cytotoxicity. This non-oriented Fc configuration also allows for a greater effective cytotoxic radius compared to the oriented Fc microparticles. For this reason, all particle types in this study utilized non-oriented anti-BSA IgG to initiate the complement system.

1.4 Bacterial Strains and Gram Classification

1.4.1 Gram Classification and Complement Recognition

By convention, bacteria are classified according to cell wall composition, as evidenced by Gram staining (**Figure 1.3 A**). Almost all possess a peptidoglycan layer comprised of alternating N-acetylglucosamine (GlcNAc) and N-acetylmuramic acid polysaccharide chains (MurNAc) [28]. Gram-negative bacteria display an inner and outer phospholipid membrane separated by a thin peptidoglycan layer (1-7 nm) [28]. The outer membrane is of particular significance as it contains the glycolipid lipopolysaccharide (LPS). Gram-positive bacteria have a single phospholipid membrane coated by relatively thick peptidoglycan (20-80 nm). Gram-positive peptidoglycan is often attached to teichoic acids (wall teichoic acids, WTAs) and the peptidoglycan may be bound to the underlying membrane via lipoteichoic acids (LTAs). Although peptidoglycan potently triggers complement activation [53], it is usually buried beneath polysaccharide chains (Gram-positive) or the outer membrane (Gram-negative), so complement initiators must recognize outfacing moieties. A thorough summation of targets and recognition molecules for both Gram classification is depicted in **Figure 1.3 B**. MBL binds LPS displayed by Gram-negative bacteria [54] as well as Gram-positive WTA [55]. Ficolins are distinguished by their ability to recognize acetyl groups, such as those of GlcNAc, as well as an array of sugars [28]. This recognition of GlcNAc may allow for peptidoglycan binding on Gram-positive bacteria. C1q may bind via the traditional IgG cluster/single IgM, or via pentraxins such as SAP and CRP. Notably, SAP can bind carbohydrate moieties in both Gram-positive

(peptidoglycan) and Gram-negative bacteria (LPS) [56]. C1q may also bind independently to several outer membrane constituents in Gram-negative bacteria [28, 57] as well as lipid A of LPS [29]. The alternative pathway has historically been viewed as a means of amplification rather than a means of detection, but there is evidence that properdin (or Factor P), a plasma protein that aids in the formation of the alternative pathway C3 convertase, binds the LPS of particular Gram-negative strains, initiating the cascade [58]. Of relevance to our application, the classical pathway in Gram-negative *E. coli* strains is investigated (C1q-mediated), and although we did not determine the influence of the lectin and alternative pathways, they are most likely involved.

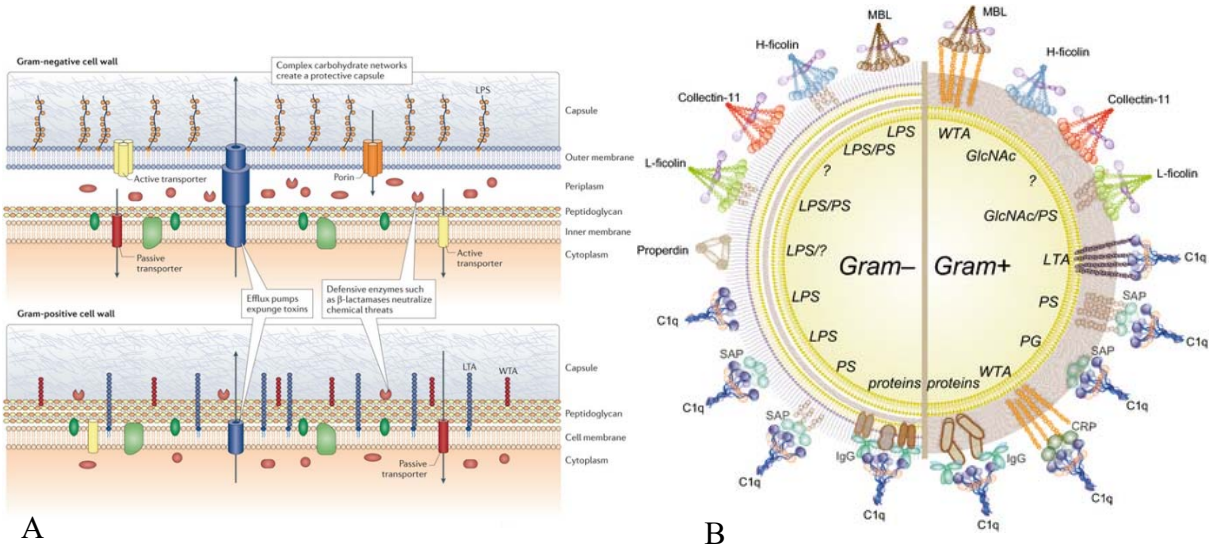

Figure 1.3: (A) Cell wall structure and composition of Gram-negative and Gram-positive bacteria. Figure adapted from [59] (B) Recognition molecules of the central compement system pathways and their association with Gram-negative and Gram-positive strains. These include those of the alternative pathway (properdin), lectin (MBL, ficolins collectin-11), and the classical pathways (C1q). Key: LPS, lipopolysaccharide; PS, polysaccharides; WTA, wall teichoic acid; GlcNAc, N-acetyl glucosamine; LTA, lipoteichoic acid; MBL, mannose-binding lectin; SAP, serum amyloid P; CRP, C-reactive protein; IgG, immunoglobulin G. Figure from [28].

1.4.2 Escherichia coli

E. coli is a facultatively anaerobic, Gram-negative bacterium naturally-occurring in the intestinal flora of humans and other warm-blooded animals. Given the ease and minimal expense with which it is cultured in the laboratory, it is of longstanding use as a model organism in microbiology. The species is massively diverse; only 20% of sequences in a typical *E. coli*

genome are conserved amongst all unique subgroups [60], termed strains. Strains can be further differentiated irrespective of evolutionary lineage by the expression of particular surface antigens, known collectively as the serotype. The main *E. coli* antigens are the O-antigen, a component of the outer lipopolysaccharide layer, the K-antigen, found in the capsule, and the H-antigen, located in the flagellin [61] (**Figure 1.4 A**). Due in part to recognition of these antigens by the humoral immune response of the host, *E. coli* are susceptible to complement mainly via the alternative and classical pathways [62].

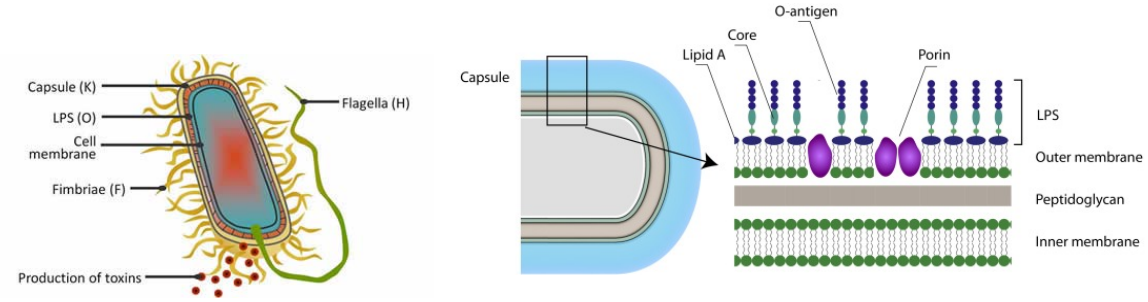

Figure 1.4: (A) *E. coli* serotype antigens used in strain classification. Figure adapted from (Université de Montreal EcL) (B) Representative Gram-negative cell wall structure, indicating the positions of lipid A and the O-antigen within the outer membrane. Figure adapted from [63].

As *E. coli* continuously evolve through gene duplication, mutation, conjugation (horizontal gene transfer), and bacteriophage-mediated transduction, pathogenic strains have diverged. Most notable of these is *E. coli* O157:H7, which is included in this study. *E. coli* O157 is frequently the causative agent in outbreaks of foodborne illness, and infection may be characterized by severe abdominal pain that in some patients can progress to hemorrhagic diarrhea, with mild or no fever [64]. Infrequently (5-10% of cases), infection may progress to hemolytic uremic syndrome (HUS) [65, 66], which can result in potentially life-threatening kidney injury. The majority of HUS cases in the United States are due to *E. coli* O157, and young children, the elderly, and the immunocompromised are most at risk. Critical to its pathogenicity are numerous virulence factors, namely the secretion of hemolysin and Shiga toxins 1 and/or 2 [65]. Shiga toxins released in the gut bind to and induce cell death in commensal bacteria, susceptible cells of the endothelium upon translocation across the intestinal

epithelium, and in renal tubular and glomerular epithelial cells [67, 68]. Upon cell entry, the toxin inhibits tRNA binding to ribosomes, occluding protein synthesis [69]. Shiga toxin is encoded by a prophage integrated in the *E. coli* O157:H7 genome, which may be triggered by antibiotic use [70]. For this reason, treatment with antibiotics is contraindicated [71]. As extensive complement activation is associated with both E. coli O157 infection and Shiga toxin bioactivity in the progression to HUS [72-74], the best-suited therapeutics will likely aim to impair rather than encourage complement formation [75]. Interestingly, *E. coli* O157 produces several virulence factors in addition to Shiga toxins that allow for complement evasion. The serine protease EspP cleaves C3/C3b and C5 [76] and the metalloprotease StcE cleaves C1-esterase inhibitor, increasing its capacity to neutralize C1s (preventing classical pathway initiation) and the mannose-associated serine proteases of the lectin pathway [74]. In addition, StcE can bind to both O157 and host surfaces, tethering C1-esterase inhibitor to shield the pathogen. For these reasons, although a complement-based therapeutic might be unsuitable for O157, demonstrating selectivity with the targeted microparticles might more effectively bypass complement subversion, and provide insight for future therapeutic strategies.

E. coli J5 is termed a rough mutant of serotype O111:B4 as the O-antigen component of its lipopolysaccharide is absent, thereby exposing the more evolutionarily conserved core and lipid A of the lipopolysaccharide [77] (**Figure 1.3 B**). As such, this strain was of considerable clinical interest for vaccination to prevent bacteremia and sepsis caused by a host of Gram-negative bacteria [78-80]without the need for antibiotics, which may incite endotoxin release. In this study, J5 was selected as a model bacterium given its complement sensitivity and the array of commercially-available monoclonal antibodies to this strain.

1.5 Motivation

Antibiotics of longstanding clinical use are nonspecific, resulting in toxicity to commensal bacteria that are central in preventing colonization of mucosal surfaces by pathogenic

bacteria, establishing mucosal immunity, and maintaining tolerance to food antigens in the gut, among other functions [11]. Not only do these antibiotics apply selection pressure to favor more entrenched antibiotic resistance, but there is evidence to suggest that their interference with commensals may contribute to numerous pathologies.

We have previously demonstrated that the extent and orientation of IgG surface coverage modulates the complement response and affects the availability of its soluble mediators, with non-oriented, high-density IgG most favorable to cytotoxicity. In combining targeting and complement activation into a single particle, we aim to improve cytotoxicity against a sought strain, presumably by improved localization of the corresponding particle. The particles and their nomenclature are shown in **Figure 1.5** below. No strain-specific antibiotic modality currently exists for Gram-negative bacteria (antibiotics specific to *Staphylococci* are in clinical trials [Debiopharm Group]. Although the base particles are too large (1 μm) to be therapeutically practical and are not biodegradable, this study is intended as a proof-of-concept measure to demonstrate that the nonspecific complement system may be targetable.

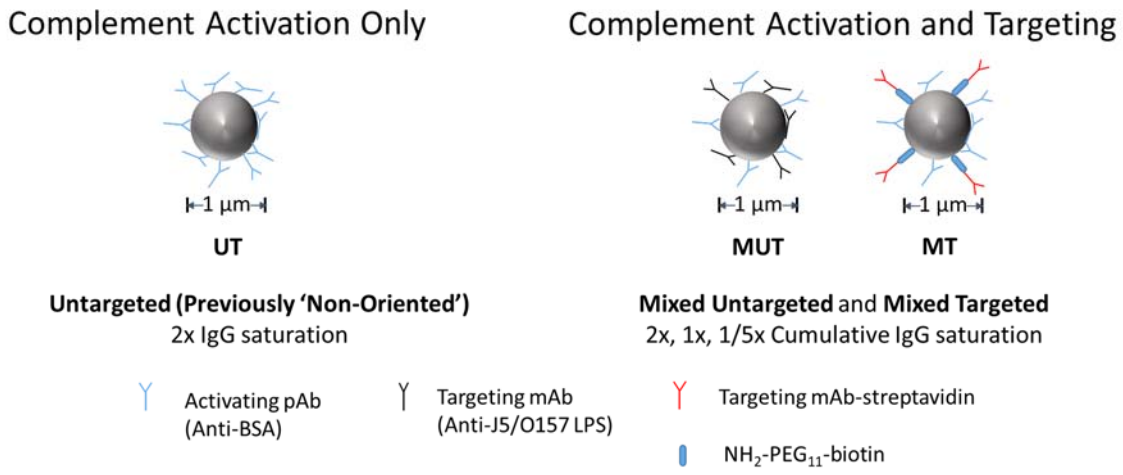

Figure 1.5: Particle panel detailing each variant and what each contributes to cytotoxicity.

1.6 Objectives

This research aims to demonstrate a more targetable platform to localize complement-mediated cytotoxicity to a sought bacterial strain. If successful, we will have developed a targeted, modular, "customizable" antibiotic that provides a tunable response with the adjustment of the initiating Fc orientation and abundance. In addition, the cytotoxic and inflammatory responses are better restricted given the targeting capacity and an inherent immune response is harnessed and can be abated by the human body's own homeostatic control.

CHAPTER 2: METHODS

2.1 Functionalization of Non-Targeted (UT and MUT) Particles

Carboxylated polystyrene microparticles 1 μm in diameter (Bangs Laboratories, Fishers, IN) were centrifuged and washed several times in PBS (5500xg, 5 min each) to remove buffers and preservatives such as sodium azide from the manufacturer's formulation. These polystyrene microparticles were selected as the base material as they are highly uniform, their IgG conjugation and saturation schemes are standardized as previously determined by the manufacturer (Bangs Labs Technotes 204 and 206), and we have previously utilized them for complement modulation [33, 50, 52]. Our previous work has investigated the impact of both particle Fc density [33, 52] and orientation [33] in augmenting or diminishing the localized classical complement response, and we have determined that cytotoxicity is most strongly associated with high Fc density and randomized display. To form the untargeted particles (UT), 2 mg/mL polyclonal rabbit anti-BSA (ThermoFisher, Waltham, MA) was added in sufficient volume to provide 2x particle surface saturation and allowed to adsorb nonspecifically, as previously reported [33]. The mixed untargeted particles (MUT) were synthesized similarly, with the addition of a mouse monoclonal antibody specific to one of the test strains (either anti-*E. coli* O157 IgG or anti-*E. coli* J5 IgG from Abcam, Cambridge, MA) at half the amount recommended by the manufacturer for various extents of particle saturation (2x, 1x, and $\frac{1}{5}$x) for a single IgG (Bangs Labs Technote 205). For example, 2x anti-O157 MUT received IgG volumes suggested for the 1x saturation extent of each antibody (6.3 μL anti-O157 and 7.6 μL anti-BSA).

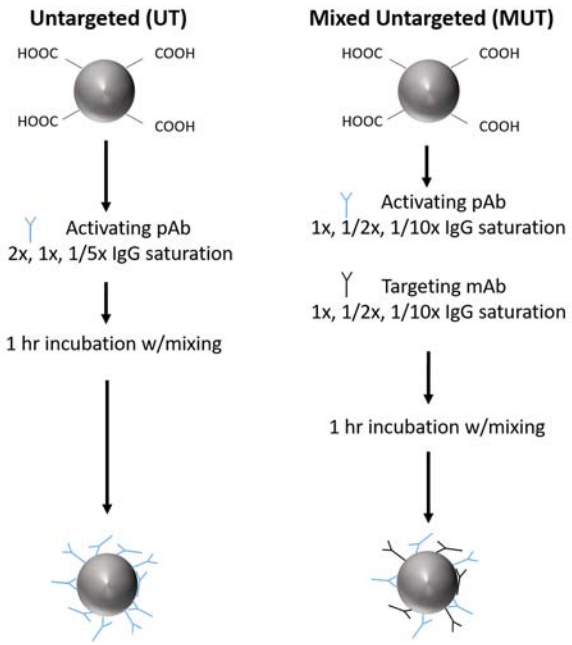

Figure 2.1: Flow diagram of UT and MUT particle functionalization. For convienience, the multiple wash steps between the addition of each component were omitted.

2.2 Biofunctionalization of Mixed Targeted (MT) Particles

To determine any benefit of targeting without hemispherical segregation of binding, mixed targeted particles (MT) were developed, which differ from the UT and MUT in that the binding antibody is conjugated such that the antigen-binding fragment (F_{ab}) projects outward. This was accomplished via the streptavidin-biotin interaction, in which the streptavidin-conjugated targeting antibody is mated to the biotin-terminated crosslinker NH_2-PEG-biotin. But first the carboxyl surface must be activated such that the crosslinker binds in the proper orientation.

EDC is a water-soluble carbodiimide crosslinker that primes exposed carboxyl groups, creating an amine-reactive ester intermediate for covalent linkage to a protein containing a primary amine group [81]. For optimal stability, EDC must be used within an environmental pH between 4.0-6.0 [81]. Also, EDC is highly hygroscopic, so solutions must be freshly prepared

and utilized immediately. Here, 25 μL of 0.2 mg/mL EDC (ThermoFisher Scientific, Waltham, MA) in pH 6.0 coupling buffer (Polysciences, Warrington, PA) was added to each particle pellet of approximately $3.6*10^8$ particles, which were then incubated at room temperature for 15 minutes prior to protein conjugation. Immediately afterwards, the tubes were centrifuged and the supernatant was aspirated for the addition of NH_2-PEG-biotin.

EZ-Link NH_2-PEG_{11}-biotin (ThermoFisher Scientific, Waltham, MA) was selected given the long PEG spacer arm, which would minimize steric hindrance amongst both the binding and activating moieties. The concentration required for half saturation of particles was determined via titration and labeling with allophycocyanin (APC)-labeled streptavidin. Briefly, 39 mg EZ-Link NH_2-PEG_{11}-biotin was dissolved in 1 mL coupling buffer (50mM) and diluted serially to 62.5 μM. From these solutions, 100 μL in coupling buffer was added to EDC-activated particle pellets as described above. The tubes were then incubated for 2 hr with end-over-end mixing. Next, 5 μL of the particle solution was incubated with 3 μL 0.2 mg/mL APC-streptavidin in PBS for 1.5 hr and then diluted 1:100. Flow cytometry was conducted (BD Accuri C6, BD Biosciences, San Jose, CA) with median fluorescence intensity (MFI) determined via FlowJo v10.0 software (FloJo LLC, Ashland, OR). Amine-PEG-biotin saturation was determined as the point of maximum MFI, or 5 mM. For particle functionalization, 2.5 mM of NH_2-PEG-biotin was added to EDC-activated particle pellets as previously described. Various amounts of streptavidin-conjugated antibody to a particular bacterial strain and anti-BSA were then added at 2x, 1x, and $\frac{1}{5}$ x particle saturation extents.

2.2.1 Antibody Conjugation to Mixed Targeted Particles

To affix the targeting antibodies to the biotinylated gold hemisphere, mouse monoclonal antibodies anti-*E. coli* O157 IgG and anti-*E. coli* J5 IgG (both from Abcam, Cambridge, MA) were conjugated with streptavidin using Lightning-Link® Streptavidin Kits (Innova Biosciences, Cambridge, UK) according to the manufacturer's instructions. They report that the kit has been designed such that each antibody can bind a maximum of three streptavidin molecules. Not only does this multivalent display improve the likelihood of biotin binding, but as the kit functions by activating amines, this reduces concerns of surplus streptavidin conjugation, which might otherwise prevent an upright IgG orientation. Anti-*E. coli* J5 was first concentrated to 1mg/mL for use with the streptavidinylation kit via 3 kDa or 10 kDa MWCO spin filters (EMD Millipore, Billerica, MA). This filtration technique also allows for the removal of the antimicrobial sodium azide contained in the formulation, which would otherwise impede conjugation to amines and confound cytotoxicity results.

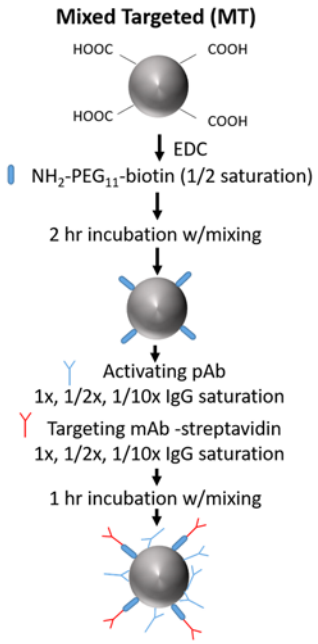

Figure 2.2: Flow diagram of MT particle functionalization. For convienience, the multiple wash steps between the addition of each component were omitted.

2.3 Particle Labeling for Counts and Labeling Determination

To verify IgG adsorption or conjugation to each particle type, 5 μL of particle solution was stained with Dnk anti-Rb Dylight 650 (Abcam, Cambridge, MA, bound anti-BSA) and Dnk anti-Ms Alexa Fluor 488 or Gt anti-Ms FITC (both ThermoFisher, Waltham, MA, bound Ms targeting antibodies), with the exception of the UT particles, which were stained with the anti-Rb secondary alone. The amount of secondary antibody was adjusted according to the primary IgG saturation extent and primary IgG concentration used to form the particles, as previously determined [52]. Secondary antibodies were reacted with the particles in 50 uL total volume with end-over-end mixing in the dark for 1 hr. The particles were then centrifuged (5500xg, 8 min), aspirated, and resuspended to 500 uL in PBS (1:100 dilution) for analysis via flow cytometry.

2.4 Flow Cytometry for Particle Counts and Labeling Verification

To determine particle counts for binding and cytotoxicity experiments as well as to verify protein conjugation, the Accuri C6 flow cytometer (BD Biosciences, San Jose, CA) and its integrated analysis software were utilized. Bare polystyrene particles were used to identify the particle population gated on FSC vs SSC, for a total of 300,000 events. The intensity distribution for 100,000 events was determined for each particle type and extent of IgG coverage in the FL1 (Alexa Fluor 488) and FL4 (Dylight 650) channels. Labeled particles were those with more pronounced fluorescence intensity in FL4A or both FL4A and FL1A with respect to the unfunctionalized control, as appropriate. To determine counts, the overlap of the particle gate and the population with the sought fluorescence configuration was determined, and the count was considered the quotient of this population and the volume of sample analyzed. All analyses,

median fluorescence determination, and plotting was completed in FlowJo v10 software (Ashland, OR).

2.5 Bacterial Strains

E. coli serotypes O157:H7 (strain CDC EDL 933, ATCC® 43895™) and J5 (mutant of serotype O111:B4, strain ATCC® 43745™) were purchased from the American Type Culture Collection (Manassas, VA). All strains were used as received, cultured in Luria-Bertani (LB) broth and plated on LB agar (both Fisher Scientific, Waltham, MA).

2.6 Serum Collection and Heat Inactivation

Blood was donated by a single healthy volunteer to minimize batch variability. Blood was first allowed to clot at room temperature for 45 min. To isolate serum, the blood was centrifuged at 1000 xg at 4°C for 15 min. Residual platelets were removed by pelleting upon centrifugation at 900 xg for 5 min, with the serum decanted as the supernatant. The serum was then divided to aliquots stored at -80° C. Serum was thawed immediately before use.

To produce heat-inactivated serum, 200 μL of normal human serum was incubated for 2 hr at room temperature with approximately $9 \bullet 10^6$ 4 μm Protein G – labeled particles developed in our lab. The particles were then removed by pelleting at 6100xg for 5 min. Next, the aliquots were incubated in a water bath set at 56°C for 30 min to denature complement proteins. The tubes were then left to cool to room temperature before overnight storage at 4°C. To remove any residual IgG precipitate formed during heat inactivation, the serum was centrifuged at 800xg for 30 min and the supernatant recovered. This fully-processed heat-inactivated serum was stored in aliquots at -80°C until use.

2.7 Cytotoxicity Analyses

Cytotoxicity was determined via manual colony counting of serially diluted mixtures of bacteria in LB broth, particles, and serum. Approximately 500,000 bacteria (as determined by absorbance, OD_{600}) suspended in 10 µL of LB broth were combined with various numbers of particles in 30 µL PBS, according to the sought particle-to-bacteria ratio. LB Broth was then added, followed by serum to initiate the complement cascade. Serum was diluted in broth such that it comprised roughly 10% or 1% of the total mixture volume of 125 µL – 0.2 (J5) - 1% (O157) serum allowed for discernment of differences among particle conditions after plating, as more concentrated serum could completely preclude colony growth. To verify that any cytotoxic effect was complement-mediated, functionalized 2:1 anti-J5 microparticles and bacteria were incubated with serum depleted of IgG and heat-inactivated, and a non-functionalized particle and untreated bacteria condition was included.

Upon serum addition, sample tubes were incubated for 3 hr at 37°C, followed by tenfold dilution in LB broth 5-6 times such that colony numbers suitable for manual counting could be generated. A 10 µL aliquot of the mixture was added to 100 µL broth, mixed and this process was repeated sequentially. The fifth and sixth dilutions were kept for plating; four 10 µL droplets were placed on LB agar plates. The plates were then incubated at 37°C for 16 hr, photographed and colony forming units counted. Bacterial lawns were given a value of 160 colonies, and incomplete lawns 120. Cytotoxicity was determined as the difference between the average colony count per condition compared to the bacteria in broth control. Statistics were determined via a one-way ANOVA with Tukey post-hoc test via GraphPad Prism 6 software (La Jolla, CA).

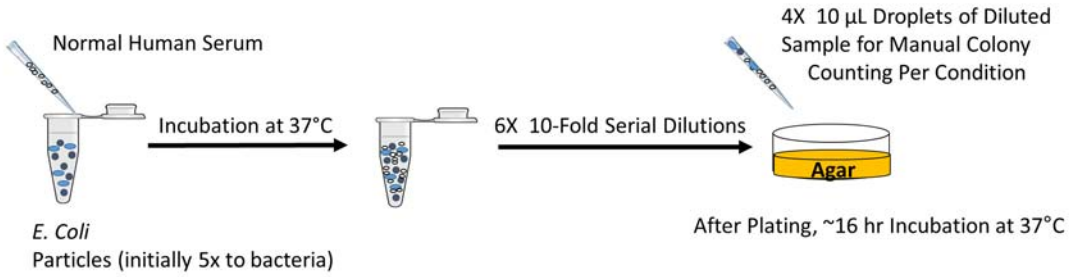

Figure 2.3: Schematic overview of plating cytotoxicity experiments.

2.8 Confocal Microscopy Analysis of Particle Targeting

Confocal microscopy (Zeiss Elyra PS.1/LSM 780, Zeiss, Oberkochen, Germany) was implemented to verify binding between particles and their target strains. Glass microscope slides were first sonicated in ethanol for 30 min, followed by washing in DI water. To adhere bacteria to the surface, 5 µL of 1.66 mg/mL Cell-Tak in 5% acetic acid (Corning Life Sciences, Tewksbury, MA), a formulation of mussel adhesion proteins, was mixed into a 60 µL droplet of PBS and incubated in the dark for 25 min. Approximately $5 \bullet 10^6$ bacteria (as determined by absorbance, OD_{600}) were stained in 100 µL PBS via the LIVE/DEAD BacLight Bacterial Viability Kit (ThermoFisher Scientific, Waltham, MA) at 3 µL per sample. To remove excess dye, the bacteria were washed twice in PBS (6000xg, 10 min each). Next, 50 µL of the bacterial solution was added to the Cell-Tak region and allowed to attach in the dark for 25 min. Unattached bacteria were removed by aspiration. Particles ($5 \bullet 10^6$) were incubated with Dnk anti-Rb Dylight 650 with end-over-end mixing for 1 hr and then washed once in PBS (5500x g, 8 min) and resuspended to 25 µL in PBS. In this way, the particles could be identified by tagging the bound anti-BSA with lessened impediment to binding the bacteria. Particles were then added to the region and allowed to bind for 25 min. Unattached particles were then aspirated. A droplet

of mounting media (SlowFade Diamond, ThermoFisher, Waltham, MA) was placed over the region, a coverslip was applied, and the edges sealed with nail polish. The slides were cured at room temperature for 20 min before placing in an opaque box at 4°C overnight. Slides were imaged the following day.

Differences in binding proclivities amongst the particle types were compared by manually counting and determining the ratio of binding events to the number of total particles in 10 separate frames acquired at the same zoom (0.7) set in the Zen 2012 software. To reduce crosstalk across fluorescence channels, spectral imaging (Lambda mode) was employed.

2.9 iC3b and TCC ELISAs

To assess the effect of particle IgG display in variations in complement progression, complement mediators were quantified at the molecular level. Activation products iC3b and TCC upon serum exposure both in supernatant and adsorbed to the particles were determined by ELISA as described in [33]. Briefly, approximately $2 \bullet 10^7$ particles in 86 µL PBS was added to 14 µL pooled normal human serum (Pierce, ThermoFisher Scientific, Waltham, MA) and incubated for 1 hr at 37°C to ensure robust complement activation. To isolate complement fractions in the supernatant from those absorbed to the particles, the particle solution was then centrifuged at 6000xg for 8 min and the supernatant separated. Both the particle pellet and supernatant were each diluted 1:200 and divided to the wells of a microassay plate included as part of the MicroVue iC3b or CH50 Eq ELISA kits (both Quidel, San Diego, CA). The CH50 Eq ELISA kit provides a proxy measure of total TCC as CH50 equivalent units per microliter. The CH50 unit corresponds to the test serum volume needed to lyse 50% sheep erythrocytes

sensitized to rabbit IgM, and is a standard method by which complement activation is determined.

CHAPTER 3: RESULTS

3.1 Verification of Different Particle Classes with Flow Cytometry

Flow cytometry was conducted to verify particle labeling and increasing surface coverage with larger amounts of IgG. After isolation of the particles by forward scatter – side scatter, this population was analyzed for fluorescence in the channels corresponding to Gt anti-Ms FITC or Dnk anti-Rb Alexa Fluor 488 (FL1) and anti-Rb DyLight 650 (FL4). Fluorescent signal above the background on a logarithmic scale (as determined from unfunctionalized particles) was considered to indicate labeling, with an increase in median fluorescence intensity in each channel suggesting greater IgG labeling extent. Median fluorescence intensity was selected as the labeling metric as it less sensitive than the mean to the skewness of flow cytometry data. Particles counts used in subsequent analyses (plating cytotoxicity experiments, confocal, etc.) were determined from dual-labeled particle concentrations. As we have previously characterized the labeling of the UT and the staining procedure was unchanged, the UT labeling results are not shown.

3.1.1 Randomized IgG Particle (MUT) Labeling

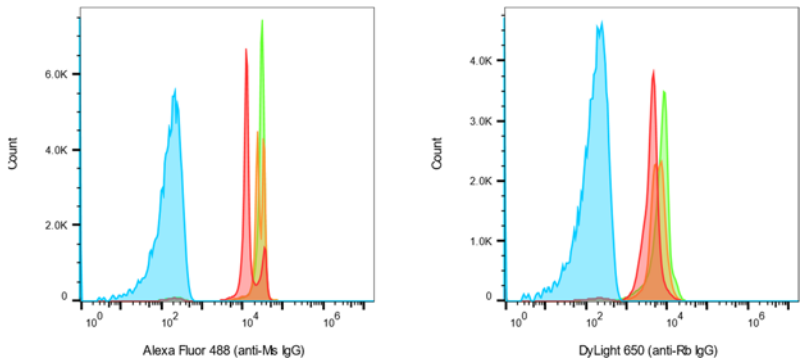

A

	Sample Name	Subset Name	Count	Median : FL1-A	Median : FL4-A
	A01 1 to 1000 Unfunctionalized.fcs	Particles	139029	153	149
	A02 1 to 100 1 to 5x O157 MUT.fcs	Particles	49125	12876	4214
	A03 1 to 100 1x O157 MUT.fcs	Particles	40174	25370	5856
	A04 1 to 100 2x O157 MUT.fcs	Particles	47495	29127	7563

B

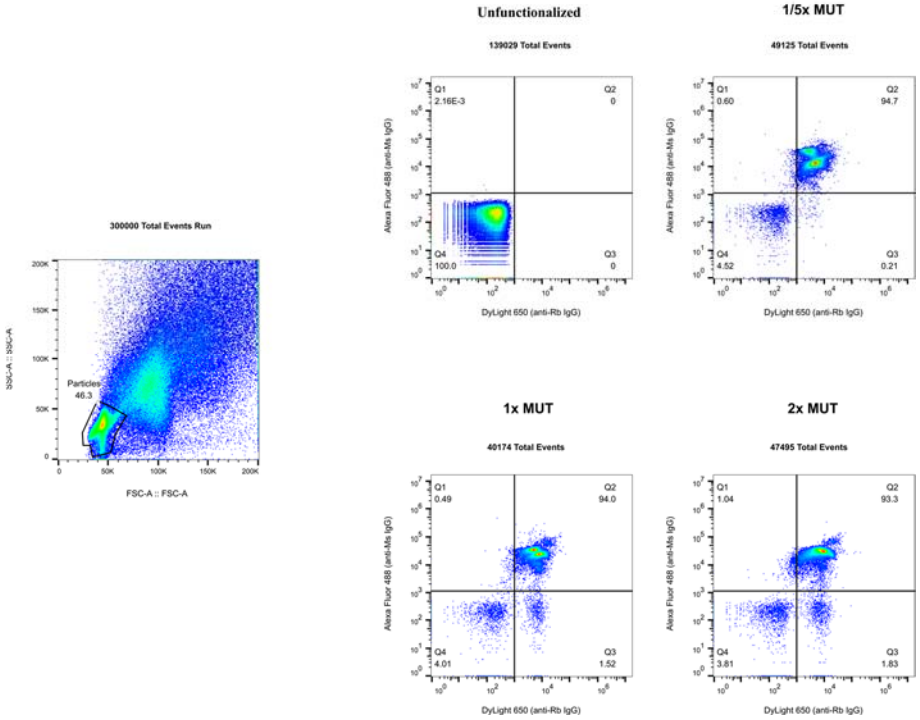

Figure 3.1. (A) Histogram overlays of O157 median fluorescence intensity with increasing IgG surface coverage and (B) dual-signal fluorescence intensities and subpopulation proportions of J5 MUT particle variants.

3.2.1 Targeted IgG Particle (MT) Labeling

From the representative labeling experiments below, median fluorescence increases with theoretical IgG surface coverage for both the J5 and O157 MT. Both partition more fully to the dual-labeled type (upper right quadrant) with increasing IgG surface coverage, yet the dual-labeled subpopulation is minimal for the $\frac{1}{5}$x J5, though it increases substantially thereafter. The remaining $\frac{1}{5}$x J5 MT subpopulations (unlabeled, and singly-labeled with anti-BSA or anti-J5) contain roughly equal proportions of the particles. Perhaps the difference in the extent of anti-J5 versus anti-O157 IgG is due to charge differences –adsorption kinetics to a solid surface are

markedly affected by the charge of the protein and the surface charge density of the substrate [82]. The carboxylated polystyrene particles are negatively charged [83], but their surface change density is altered by ongoing anti-BSA adsorption and the attachment of the streptavidinylated antibacterial IgG to the crosslinker. The O157 IgG may be more robust to this process, and the relation of IgG charge and surface density pre- and post-crosslinker addition warrants further investigation.

The $\frac{1}{5}$x O157 MT display a more pronounced partition into the anti-BSA labeled subpopulation (lower right quadrant) at the lowest IgG concentration, but there is then a substantial shift to the dual-labeled subpopulation with increasing IgG. This increase in secondary antibody signal for the O157 MT is expected with an increase in available epitopes, suggesting increased labeling at higher primary IgG concentrations in combination with the median fluorescence results.

A

J5 MT

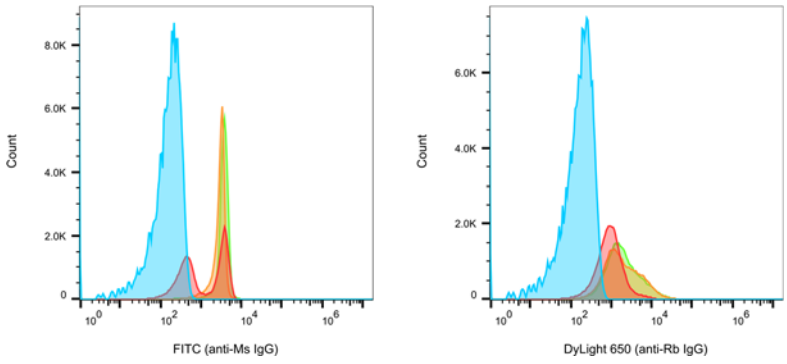

	Sample Name	Subset Name	Count	Median : FL1-A	Median : FL4-A
	A01 PP 1 to 200 Unfunctionalized.fc	Particles	230422	152	149
	A05 1 to 100 1 to 5x J5 MT.fcs	Particles	52430	861	911
	A06 1 to 100 1x J5 MT.fcs	Particles	49472	3095	1656
	A07 1 to 100 2x J5 MT.fcs	Particles	50223	3701	1739

B

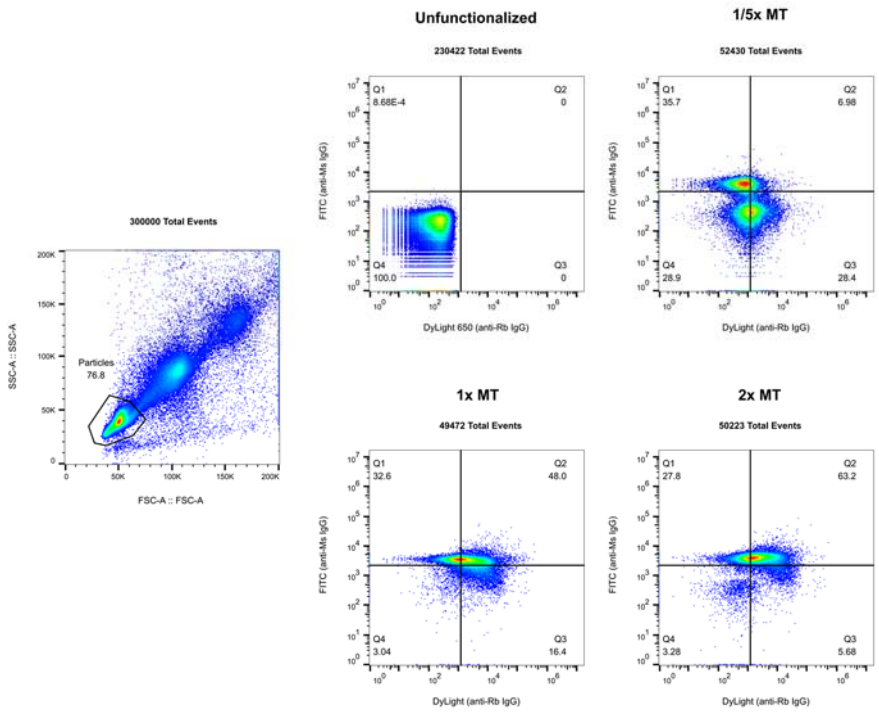

Figure 3.2. (A) Histogram overlays of median fluorescence intensity with increasing IgG surface coverage and (B) dual-signal fluorescence intensities and subpopulation proportions of J5 MT particle variants. Note that the J5 and O157 MT particles were run in the same experiment, so the unfunctionalized control is shared.

O157 MT

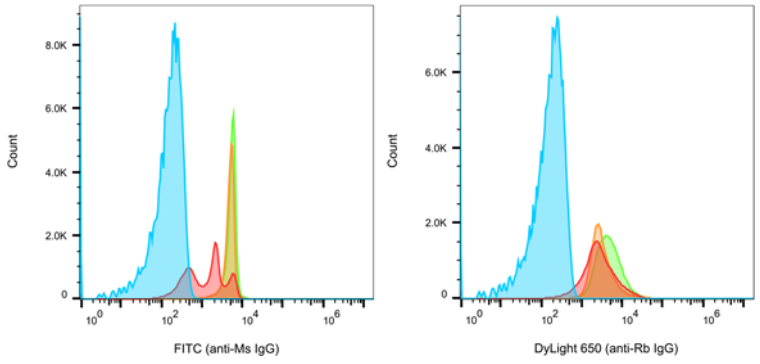

A

Sample Name	Subset Name	Count	Median : FL1-A	Median : FL4-A
A01 PP 1 to 200 Unfunctionalized.fcs	Particles	230422	152	149
A02 1 to 100 1 to 5x 0157 MT.fcs	Particles	46319	1454	2506
A03 1 to 100 1x 0157 MT.fcs	Particles	39835	5039	2830
A04 1 to 100 2x 0157 MT.fcs	Particles	46394	5555	4425

B

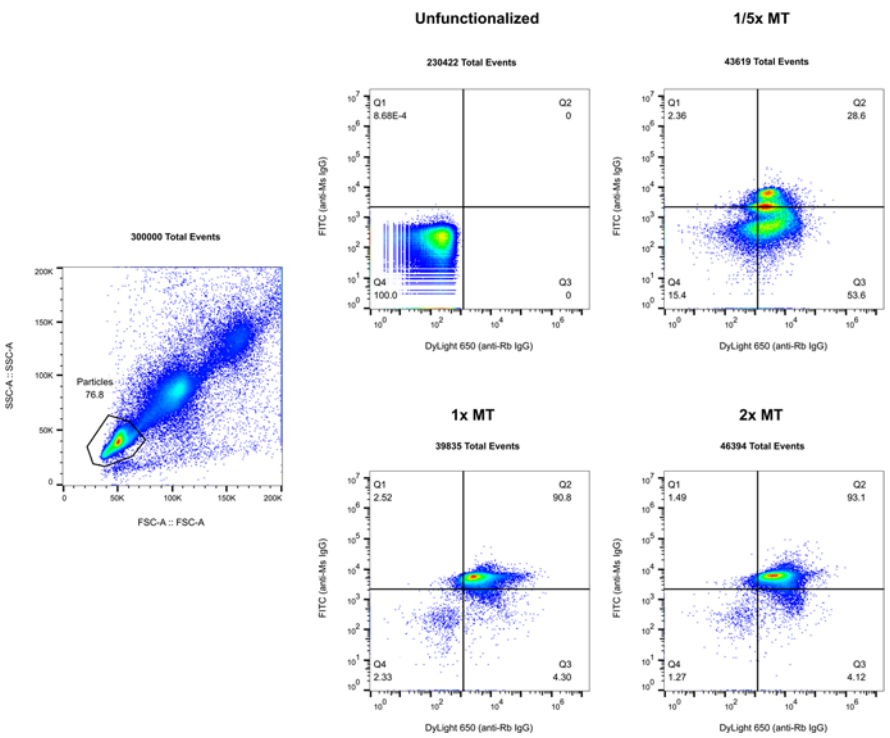

Figure 3.3. (A) Histogram overlays of median fluorescence intensity with increasing IgG surface coverage and (B) dual-signal fluorescence intensities and subpopulation proportions of O157 MT particle variants. Note that the J5 and O157 MT particles were run in the same experiment, so the unfunctionalized control is shared.

3.2 Plating Cytotoxicity Experiments

To distinguish the cytotoxic effectiveness of the particle types and any influence of surface coverage, *in vitro* plating experiments were conducted, as detailed in **Section 2.7**. Briefly, particles were incubated 5:1 with bacteria (2,500,000 particles and 500,000 bacteria), broth, and normal or heat inactivated human serum. Tubes were incubated at 37°C for 3 hr followed by serial dilution and further incubation of 10^5- and 10^6-fold dilution agar plates as these resulted in countable colony formation. Serum concentrations were determined in separate

but similar experiments with decreasing serum concentration from 5% by volume to the point at which sensitivity was evident but colony formation was still substantial.

3.2.1 Randomized IgG Particle (UT and MUT) Cytotoxicity

UT and MUT particles of increasing Fc surface coverage were evaluated to determine whether including a targeting monoclonal IgG, even if randomly adsorbed to the particles, provided any cytotoxic benefit. Only the 2x Fc saturation UT particles were evaluated as we have previously demonstrated increasing cytotoxicity with Fc saturation, with maximal effect at 2x saturation for the same anti-BSA IgG and base particles (also called 2:1 non-oriented) [33].

From **Figure 3.4**, for the 10^6-fold dilution there is some increase in antibacterial capacity against the complement-sensitive J5 with increasing Fc coverage for the MUT, but cytotoxicity is most dramatic for the 2x UT and this is only group with statistical significance ($p = .0077$) relative to untreated cells. This may be due to maximization of available Fc for complement activation – a fraction of the targeting IgG Fc is unable to bind C1q due to sterics upon binding bacteria. Additionally, the subclass composition of each IgG is important, as they vary in the extent of classical complement fixation [84]. The polyclonal anti-BSA consists of an array of subclasses whereas the monoclonal targeting IgG are all the same subclass; complement activation may be greater if certain subclasses dominate among the mixture. Given that heat inactivation of the serum combined with the 2x MUT displays minimal effect and is most like the untreated cells, complement-mediation of the effect is implied, although for such dilute serum toxicity is already limited. The unfunctionalized particles activate complement themselves, likely as C3 and C4 bind carboxylated polystyrene possibly due to electrostatic interactions [85]. Complement activation then proceeds through the alternative pathway.

By contrast, MUT is more suitable for the complement-resistant O157 strain, and although the antibacterial effectiveness is greatest for the 2x surface coverage ($p = .0053$ relative to untreated cells), whether the factors are correlated is unclear. With targeting, complement may be better localized. Surprisingly, O157 viability increases for the 1% serum only condition. However the capability of *E. coli* to persist in serum via nucleotide synthesis has been described [86], and this may occur despite complement in dilute serum. To our knowledge this has not been previously reported in O157, and instead may be due to the inherent variability in plating assays [87, 88]. As the heat inactivated serum was shown not to be significantly toxic in combination with 2x MUT against J5, it was not evaluated with O157.

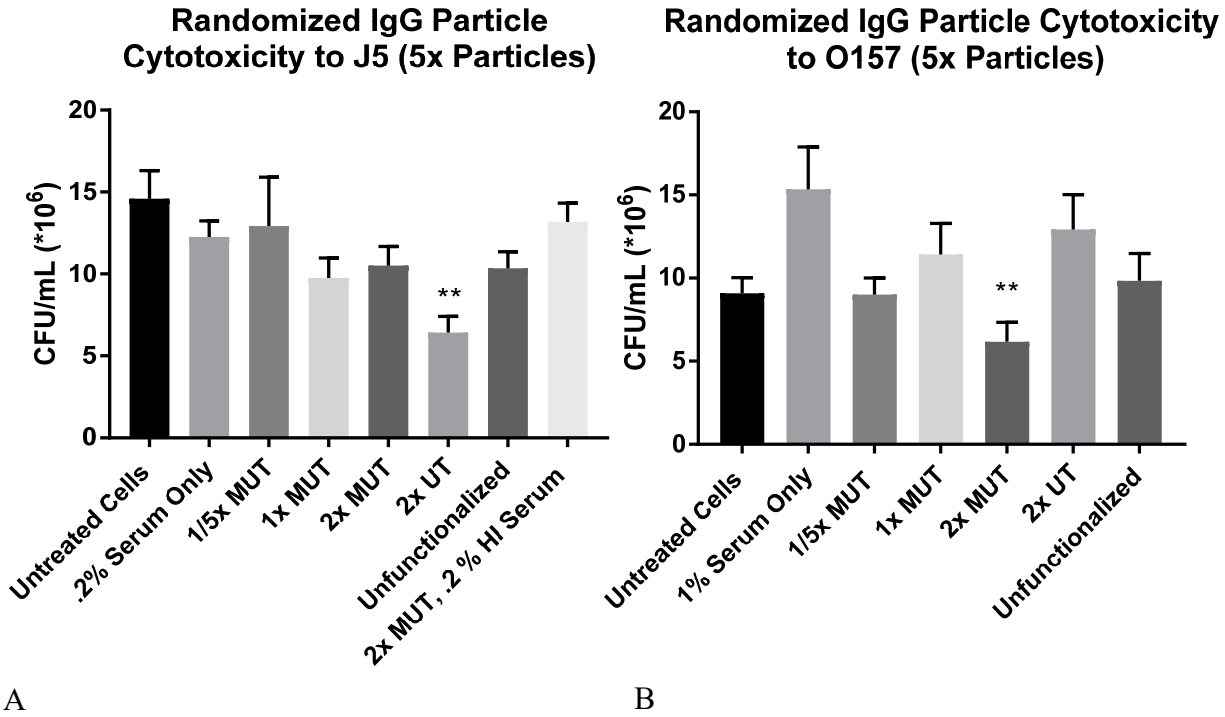

Figure 3.4. The viability of J5 (A) and O157 (B) *E. coli* following treatment with single-source normal human serum and particles of randomized Fc with varying levels of surface coverage. Particles were added at a 5:1 ratio to bacteria (2,500,000 particles to 500,000 bacteria). Results depict averages from three experiments. Error bars represent the standard error of the mean. ** $p < .01$, relative to untreated cells.

As a means to reduce this variability, colony counts for the 10^5 dilution were also recorded, as it is recommended that plates counts consist of at least 25 colonies per replicate, as there may be dubious accuracy below this threshold [89]. This occurs because CFU are contended to follow a Poisson distribution, so error is the square root of the average (USP <1227>). With plate counts less than 25, error as a percentage of the mean increases considerably [89]. From **Figure 3.5** below in which the plate counts from the 10^5 and 10^6 dilutions are compared, the most cytotoxic of the particle variants remains the same, but the change in the supposed effect of Fc coverage differs according to target strain. Although the 2x UT is again most effective against J5, cytotoxicity decreases with increasing Fc saturation, whereas the opposite appears in the 10^6 dilution, at least prior to 2x surface saturation. Regarding O157, 2x MUT still predominates, with cytotoxicity greatest for very low or very high Fc saturation, but the differences amongst the MUT are much less pronounced. Given these observations, additional trials should be conducted and an error cutoff established (ex. 20% from the mean of triplicate experiments, as suggested in a seminal paper by Breed and Doeterrer [88]). Note that the 10^6 dilution plots are extrapolated from the previous figure.

J5

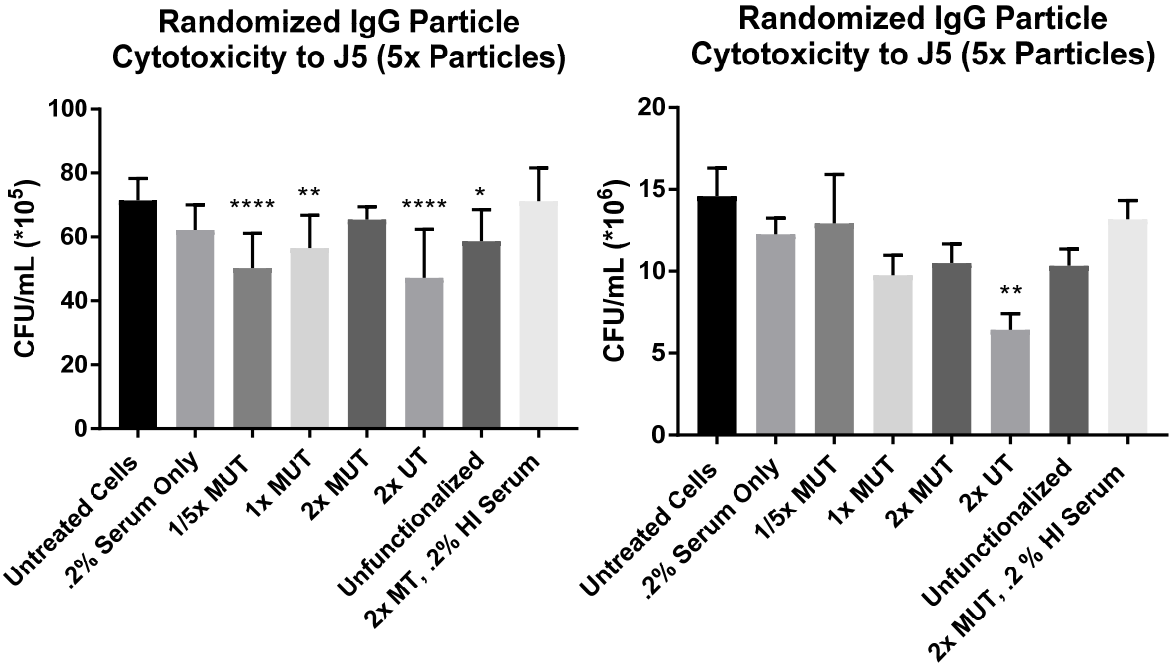

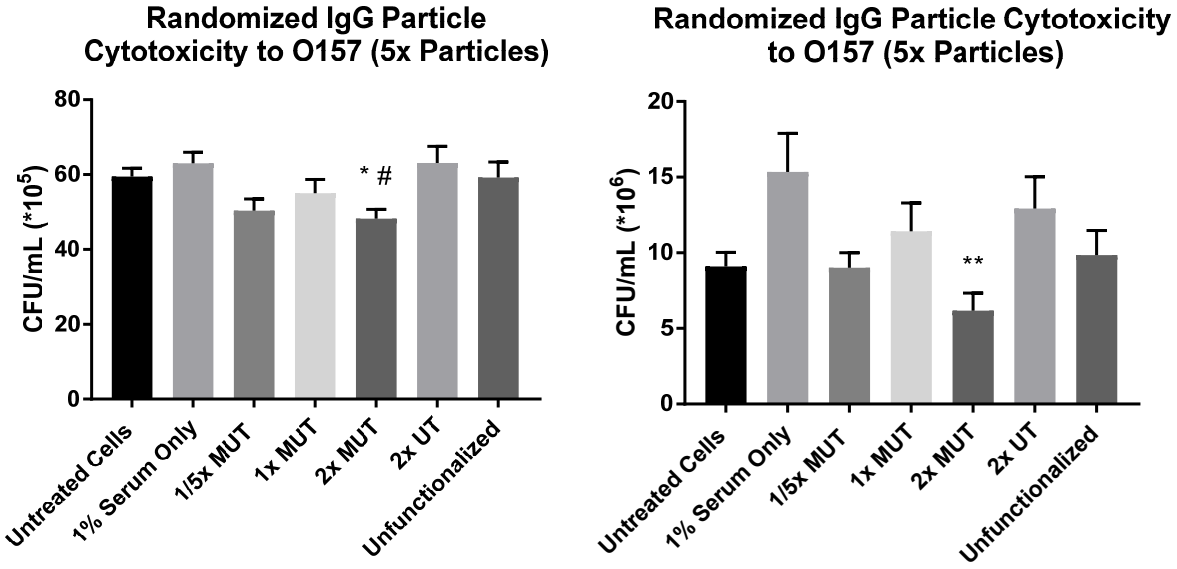

Figure 3.5. Comparison of strain viability of *E. coli* J5 (top) and O157 (bottom) by dilution after incubation with serum and MUT or UT particles of varying targeted and complement-activating IgG coverage, as applicable. All plating experiments utilized a 5:1 particle-to-bacteria ratio (2,500,000 particles to 500,000 bacteria). Note that the 10^5 dilution of the O157 particles summarizes average results from two experiments, while all others consist of three. Error bars represent the standard error of the mean. **** p <.001, ** p < .01, * p < .05, relative to untreated cells.

3.2.2 Targeted IgG Particle (MT) Cytotoxicity

We hypothesized that cytotoxicity would be improved with targeting, particularly with targeting IgG oriented such that the Fab regions project outward without steric hindrance from the complement-stimulating IgG. The MT particles differ from the MUT panel in that a crosslinker (NH_2-PEG-biotin) in theory occupies half of the available surface area per particle, with the remainder occupied by the nonspecific polyclonal activating IgG (anti-BSA). The targeting IgG is then bound to the crosslinker via the highly selective biotin-streptavidin interaction. Both antibodies were added at the same volume used to form the MUT. From **Figure**

3.6, the MT elicit little effect against either J5 or O157, even at a 5:1 particle-to-bacteria ratio. As the PEG chains of the crosslinker are not rigid, perhaps their movement blocks the binding of the IgG. For reasons discussed in the previous subsection, only the 10^5 dilution was evaluated. Particles seem to be slightly cytoprotective for J5, but any correlation with IgG density is uncertain. There is minimal improvement in O157 with increasing Fc coverage, but the variation is within the bounds of the error. The outcome of HI serum treatment for the J5 suggests that it may still activate complement substantially - perhaps there is residual heat-aggregated IgG that was not removed with the protein G microparticles. Yet O157 viability increases sharply with heat-inactivated serum relative to cells in broth alone, and this may be due to greater availability of metabolites formed by destabilized serum proteins.

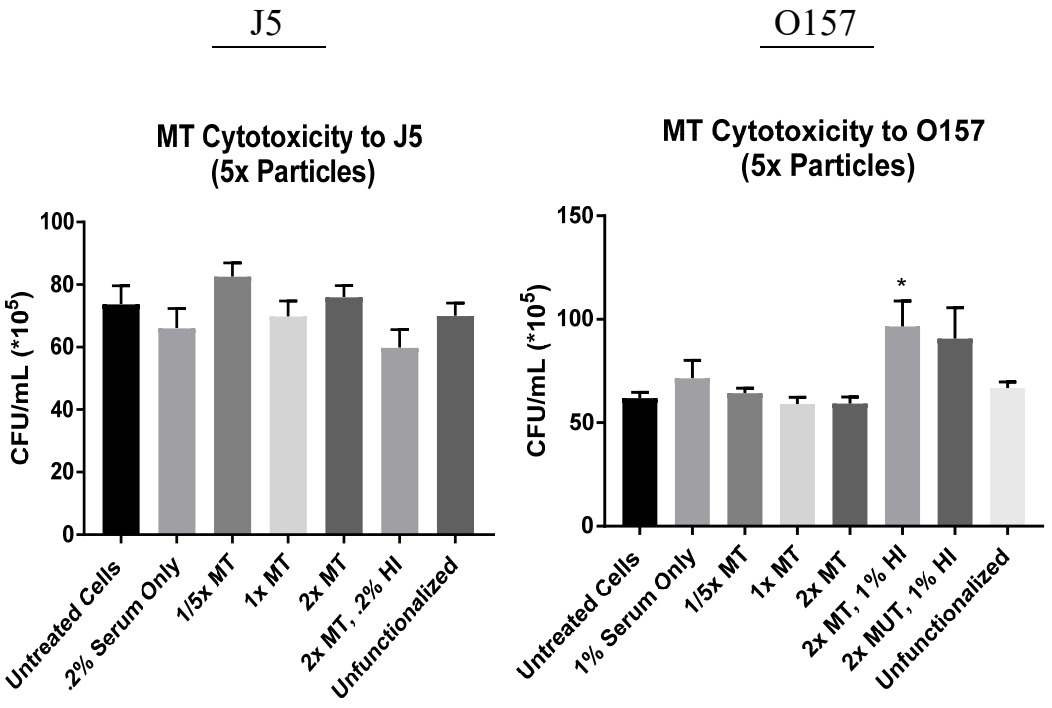

Figure 3.6. Colony counts of *E. coli* J5 and O157 treated with specified serum concentrations and MT particles of varying targeted and complement-activating IgG coverage. Particles were added at a 5:1 ratio to bacteria (2,500,000 particles to 500,000 bacteria). Results depict averages from three experiments. Error bars represent the standard error of the mean. * $p < .05$, relative to untreated cells.

3.3 Confocal Binding Assay

Given the counterintuitive cytotoxicity results, targeting proclivity differences between the UT, MUT, and MT were evaluated with a confocal binding assay, as described previously. Internally-labeled *E. coli* of the target strain was adhered to glass slides and then incubated with fluorescently-labeled 2x saturated particles of each configuration against the corresponding target strain. To distinguish particles, anti-Rb DyLight 650 specific for the anti-BSA was utilized. As variance in particle and bacterial abundance per imaging location was inevitable, binding capacity was determined to be the total number of binding events divided by the total number of particles per frame. A binding event was defined as overlap or the adjoining of particle and bacterium, and any particles in clusters were counted as individuals.

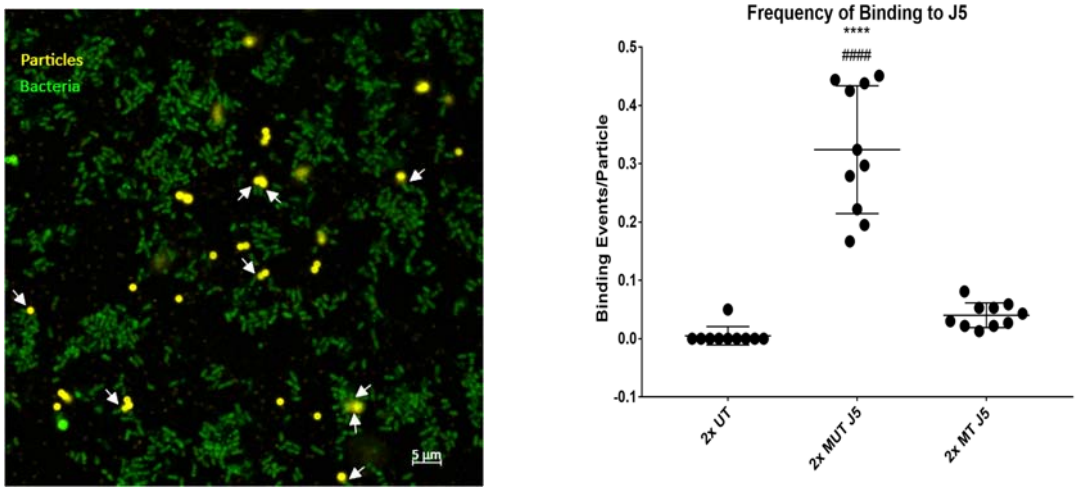

A B

Figure 3.7. (A) Representative confocal imaging frame of 2x MUT J5 against J5 bacteria. The white arrows indicate putative binding events. (B) Comparison of binding proclivities for each 2x saturation anti-J5 particle type against J5 across 10 imaging frames. The 10 imaging frames per particle type used for the analysis originate from the same slide. **** $p < .0001$ relative to 2x UT, #### $p < .0001$ relative to 2x MT J5.

The MUT drastically improves binding proclivity relative to the others, although it is variable. As expected, the UT did not bind apart from negligible off-target binding. Surprisingly,

the MT displayed minimal binding. Combined with the results of the plating experiments, this may imply that the physical properties of the crosslinker are unsuitable to allow for robust binding, or that the targeting IgG do not attach in the proper orientation, among other possibilities. To determine the theoretical half-saturation value of the crosslinker, it was apparent that the crosslinker bound (NH_2-PEG-biotin), as substantial signal was detectable with a fluorescent streptavidin conjugate (data not shown). Further, the streptavidinylated targeting IgG bound, as verified by flow cytometry in **Section 3.1**. In addition to testing the anti-O157 particle variants, future work must include another means to confirm the presence of streptavidin attached to the particles, such as an *in vitro* assay involving crosslinker-only-conjugated MT particles binding to biotinylated serum albumin adsorbed to a solid surface.

3.4 iC3b and TCC ELISAs

As we had previously demonstrated that IgG orientation may affect the abundance of complement mediators both bound to particles and available to opsonize targets in the supernatant [33], we evaluated the levels of iC3b and TCC for each O157 2x saturation particle variant post-activation. We were also interested in determining whether cytotoxicity correlated with the patterns of complement species released into the supernatant by each particle type. Both were run simultaneously using samples from the same reaction vials. Anti-O157 particles were intended as representative of dual-labeled particles. Given that the blank wells (no sample, but processed identically) displayed suspiciously high background, the iC3b ELISA results are inconclusive (data not shown). From the CH50 ELISA (proxy measurement of TCC, **Figure 3.8**), there are noticeable differences in complement sequestration and dissemination amongst the particle types. The MUT sequester the most TCC, yet prompt little TCC formation in the

supernatant. The UT and MT bind TCC at about the same extent, but slightly more TCC was present in the supernatant for the MT particles. None of the differences were substantial enough to be statistically significant.

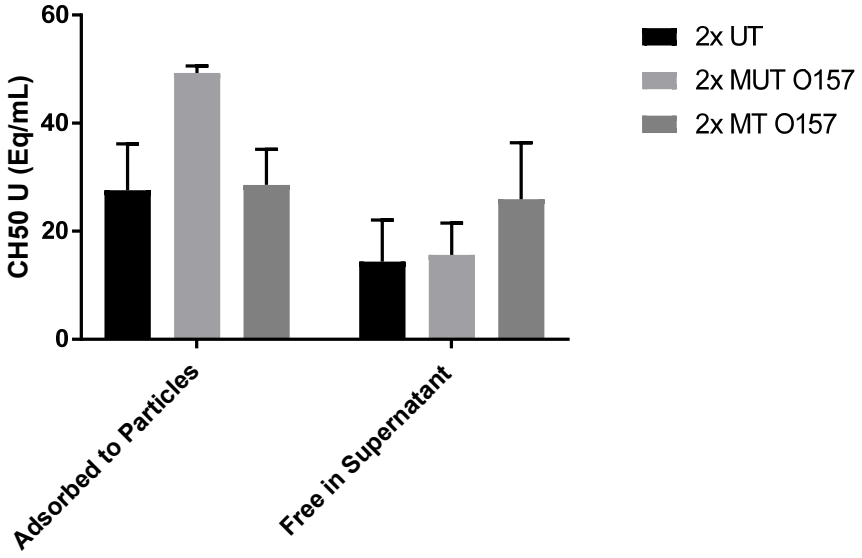

Figure 3.8. CH50 (TCC) ELISA to quantify TCC both adsorbed to particles and free in the supernatant resulting from the activation of each O157 2x saturation particle variant. After 1hr incubation at 37°C in pooled NHS, the particles were isolated and diluted 1:200 in specimen diluent (reagent included with kit) for ELISA analysis. The results display mean and standard error determined from three replicates.

There does not seem to be a clear relationship between TCC and cytotoxicity, as the MT were largely ineffective in plating experiments against either target strain. However, perhaps the MT overtake the MUT at higher doses - the particle counts used here are 8-fold that of the plating experiments. Yet there were some issues with the experimental execution itself. Heat aggregated gamma globulin (HAGG), a collection of heat-formed immune complexes, was included with the kits as a positive control, but it was not tested. Also, the slope of the concentration versus absorbance standard curve was slightly below the minimum recommended by the manufacturer (.0024 vs .0033), although the r^2 value was sufficient (>.99).

CHAPTER 4: DISCUSSION

Of the candidates, the MUT is clearly best suited to both bacterial targeting and cytotoxicity. The UT may be more cytotoxic to J5, but for any translational potential the activity of the MUT against the virulent O157 is more relevant. Surprisingly, orienting the targeting IgG does not seem to provide any benefit, although further examination of the crosslinker and its adsorption behavior should be undertaken to confirm this claim. Even more counterintuitive is that the MUT bind their target much more readily, but this must be verified for O157 strains, and to non-corresponding targets as well. The ELISA results seem to conflict with the cytotoxicity results – the 2x MUT O157, at least with anti-O157 IgG, sequesters the majority of TCC generated to the particle – but perhaps this view is incomplete, and it is the localization of complement from the binding of multiple particles that enhances cytotoxicity. The alternative pathway is unlikely to be augmented greatly by the orientation of IgG, but with certain molecular signatures (particularly hydroxyl and amine groups) more available on IgG, C3b deposition may be increased. In addition to the elements of the classical pathway, any changes in C3b, Factors B, H, and I should be analyzed. Assessment of the alternative pathway by preincubating serum with EGTA was not undertaken due to concerns about possible confounding effects of EGTA-induced *E. coli* morphology changes [90], but a different means of testing is recommended.

Pathogens generally avoid opsonization and destruction via complement by antigen modulation and blockade of complement mediator binding or by prompting their degradation once bound. For example, enzymes secreted by *Pseudomonas aeruginosa* degrade C1q as well as the various forms of the C3 opsonin [91]. Pathogenic *E. coli* may also vary their surface antigens in response to complement-induced stress – the uropathogenic strain CFT073 can downregulate

OmpC, a key surface antigen recognized by IgG in prompting the classical pathway [92]. Particular strains may possess multiple complement evasion mechanisms. *Staphylococcus aureus* displays streptococcal protein A, which inhibits classical pathway initiation by binding the antibody Fc region and inverting the molecule, thus avoiding C1q binding [93]. Another virulence factor *S. aureus* produces is staphylococcal complement inhibitor (SCIN), which binds and hinders the C3 convertase of any pathway, reducing C3b deposition [94]. Colonization may also be facilitated by the formation of biofilms, bacterial communities enmeshed in an external matrix mainly composed of polysaccharides. Typically a response to environmental stressors, biofilm incorporation provides protection from neutrophil phagocytosis, antibiotics, immunoglobulins, reactive oxygen species, and complement mediators as they are unable to penetrate deeply through the matrix [95]. Bacteria contained in the biofilm readily participate in horizontal gene transfer, and a subset can modulate genes that slow their metabolic efficiency – both of which features contribute to further antibiotic resistance [96]. With improvements to be discussed in future work, we anticipate that the MUT platform could be useful in clinical settings, despite its disappointing performance against the virulent O157. Given the considerations discussed above, a suitable bacterial target for the particle platform is preferably Gram-negative, must have a unique, accessible antigen, possess complement sensitivity, have no or limited proclivity to form biofilms, and be resistant to first-line antibiotics or display emerging resistance.

As virulent clinically-relevant bacteria innately resist complement-mediated destruction, the current MUT iteration at best may provide some benefit if used to supplement an antibiotic regimen as a sensitizing agent. Polymyxin B, a polycationic peptide antibiotic that selectively binds to Gram-negative bacteria (such as *E. coli*) via surface LPS, would be of particular interest

as it destabilizes the membrane, rendering the bacterium more sensitive to TCC [97]. Polymyxin B itself can prompt C3 and factor B secretion by monocytes [98] yet it may downregulate the neutrophil complement receptor CR3 [99]. A deacetylated form of polymyxin B, though weakly antibacterial if the activity is not totally abolished, has been noted to sensitize even serum-resistant *E. coli* strains to complement and neutrophil activity [100]. Synergy with antibiotics has been reported for clinically-relevant bacteria including *Klebsiella pneumonaie*, *Pseudomonas aeruginosa*, and *Salmonella typhimurium* [101]. In addition, the toxicities of the parent compound are avoided [100]. Pairing the MUT particles with the deacetylated polymyxin B may be suitable to effectively target multidrug resistant strains that maintain sensitivity to colistins. MUT appears to sequester the most TCC of the particle variants, and should this hold true for others mediators, particularly C5a, the MUT may be best suited to septic situations, in which complement in serum is markedly elevated [102]. However, colistin is generally used as a last resort, and resistance has been increasing steadily in *K. pneumonaie* ([103, 104] and *E. coli* [105], as a transferable plasmid has been identified [106, 107]. Instead, innate antimicrobial peptides or synthetic mimics such as the ceragenins should be utilized.

The only cathelicidin naturally-occurring in humans, LL-37, and its more potent synthetic analog, SAAP-148, have demonstrated efficacy against MRSA [108, 109] and multidrug resistant *Acinetobacter baumanii* both *in vitro* and *in vivo* [108]. Both organisms are listed by the CDC as impending 'serious' threats to public health [3]. LL-37 and SAAP-148, which are both cationic, interact with the phospholipids of both Gram-negative and Gram-positive bacterial membranes, causing them to destabilize [110]. Both have demonstrated the ability to impede biofilm formation and destroy established biofilms in antibiotic resistant bacteria [108, 111]. Although LL-37 prompts strong proinflammatory pathways [112], LL-37 and some derivatives

have demonstrated the ability to suppress the proinflammatory effects of LPS [113]. But this neutralization capacity and cytotoxicity can be reduced by serum [113]. To our knowledge, the immunological effects of SAAP-148 have not yet been reported. By pairing the MUT with LL-37 or another modified cathelicidin, this reduction in serum cytotoxicity might be overcome, more of the cytotoxic effect may be directed to the target strain, and the agents that mediate serum suppression may be identified by binding the particles. The role of LL-37 in sepsis is highly complex, however, and its interaction with complement is still being elucidated.

MUT in combination with polymyxin B/nonapeptide might merit investigation for non-bacterial drug resistant pathogens. Fungi of the *Candida* genus are opportunistic pathogens and are among the most frequent sources of nosocomial bloodstream infections [114]. The incidence of *Candida* infection is only increasing [115]. Mortality due to candidemia is significant, and patient stays in the intensive care unit are often extended several weeks relative to uninfected patients [116]. First-line treatment is often the antifungal agent fluconazole, but many common strains can be resistant –the most frequent *C. albicans*, as well as the more virulent *C. glabrata* and *C. krusi*, the latter of which can be innately resistant [117]. Clinical isolates of an emergent strain, *C. auris*, are almost exclusively fluconazole-resistant [117]. Fluconazole-resistant *Candida* are next treated with echinocandins, and *C. glabrata* in particular is increasingly resistant [118]. Patients with multidrug-resistant *C. glabrata* and *C. auris* often receive amphotericin B, which is infamous for its adverse side effects, namely a potent febrile reaction shortly after infusion, marked but reversible nephrotoxicity, hypokalemia, and anemia among others in already seriously ill patients [119].

Surprisingly, most of these disseminated *Candida* infections occur not in non-immunocompromised or neutropenic patients, but those who have received gastric surgery,

broad-spectrum antibiotics, or catheterization for parenteral nutrition or venous injections [120]. In these instances, commensal populations and anatomical barriers that might provide immune protection are disrupted. Infection with *C. albicans*, the most extensively studied, stimulates all three complement pathways [121]. *C. glabrata* and *C. krusei* are known to prompt the alternative pathway, although there is also evidence of naturally-occurring antibodies to non-*albicans Candida* in NHS, although their abundance and complement fixation capacity may be limited [122]. However, *Candida* have acquired complement evasion mechanisms – several species bind factor H [123, 124], a host-expressed complement mediator normally involved in restricting alternative pathway activation such that host cells are spared. It accelerates the breakdown of the alternative pathway C3 convertase and serves as a cofactor of factor I, which cleaves the C3b opsonin to the inactive form iC3b [42]. In addition, *C. albicans* secretes proteases that degrade bound C3b and C4b [123] and the MAC may not be able to penetrate the fungal cell wall [121]. Yet complement is still required in clearance [125], perhaps by prompting downstream adaptive responses [126]. Fluconazole-resistant *C. albicans* and *C. glabrata* do show sensitivity to polymyxin B in combination with antifungals *in vitro* [127, 128]. Given that magainin 2 - an antibiotic unrelated to polymyxin B but mechanistically similar - is also both antifungal and synergistic with fluconazole, polymyxin B may act to destabilize the cell wall, as with bacteria [129]. In this way, antifungal use is obviated, with the particle platform targeted to specific *Candida* via monoclonal antibodies to conserved cell wall components such as mannan and glucans – both incite complement [130]. At the time of writing, it appears a complement modulating approach to sensitized *Candida* has not been attempted. A further benefit to this approach is that horizontal gene transfer from bacteria to eukaryotic *Candida* such as that conferring polymyxin resistance is exceedingly rare [131].

CHAPTER 5: CONCLUSION

This work demonstrates that although there is minimal if any benefit in the mixed, targeted strategy utilizing the current crosslinker to orient the targeting antibody, cytotoxicity can be improved somewhat for the complement-resistant and clinically relevant O157 strain via nonspecific adsorption of its targeting antibody, whereas the complement-sensitive J5 is most susceptible to maximized polyclonal antibody coverage. However, this effect is insufficient to be clinically relevant, where by convention at least a tenfold improvement in cytotoxicity is sought. With modifications for clinical use and a more thorough understanding of how the two IgG types arrange and interact to maximize cytotoxicity with minimized loss of selectivity and anaphylatoxin release, the platform could be used as a first-line sensitizer to be combined with antibiotics or antibacterial peptides to slow the development of further antibiotic resistance.

CHAPTER 6: FUTURE DIRECTIONS AND RECOMMENDATIONS

There are several measures that should be considered in the near-term to optimize the current platform, with insights then extrapolated to a more clinically-translatable version. As previously mentioned, better quality control in plating is required, as results may be highly variable and counterintuitive. With deviation cut-offs determined from further repetitions and/or existing literature, trends may be more consistent. Given that plating experiments were always conducted at a 5:1 particles: bacteria ratio, constructing dosing curves would be valuable to illustrate whether the UT and MT improve upon the performance of the MUT, and if so whether the doses are reasonable for *in vivo* translation. While the TCC ELISA provided interesting information towards the design of particles that maximize TCC formation in the supernatant

rather than at the particle surface, this should be viewed in the context of other central complement mediators, namely C1q, C3b, and C5a. Lastly, although serum from the same source was used for all cytotoxicity experiments, it should be evaluated for any antibody contamination (ex. passing through a Protein A/G column) or existing properdin.

The relationship between the proportions of each antibody and cytotoxicity, selectivity, and any influence in sepsis progression must be elucidated. Perhaps the 1x saturation of each IgG (so-called 2x particles) is most cytotoxic while retaining selectivity, yet results in substantial C5a release into the supernatant. Elevated serum C5a and other anaphylatoxins such as C3a and C4a often suggest a loss of complement homeostatic control and a more serious prognosis [102, 132]. We have demonstrated that the non-oriented anti-BSA can sequester C5a from serum [33], but this needs to be evaluated for particles with the inclusion of the monoclonal targeting antibodies and/or the NH_2-PEG-biotin. Further, the targeting capability of the MT should be re-assessed with NH_2-PEG-biotin rheology to determine if a stiffer or more pliant crosslinker is suitable. The hydrodynamic character and radius of gyration of the crosslinker, if used, as well as the spacing and density of the carboxyl groups for the most effectual protein adsorption patterns must be determined to inform improved particle designs. Although protein adsorption to solid surfaces is non-uniform, the kinetics of adsorption is also affected by surface charge density [82], and this was not considered in the manufacturer's equations to determine protein amounts needed for surface saturation. To investigate both the rheology of the crosslinker as well as changes in molecular spacing on the particle surface across particle types and IgG saturation extents, atomic force microscopy (AFM) could be utilized. The Sulchek lab has considerable expertise with this tool, and we have used it previously to probe the surface of UT particles [33].

Complement fixation can be enhanced both by changing the class of the prompting IgG. IgG was selected in this study due to its ubiquitous commercial availability and previous characterization in our laboratory with the carboxylated particle base [33, 50, 52]. IgG is composed of four classes (IgG1-4), ordered by decreasing relative abundance in sera [84]. C1q binds more effectively to IgG1 and IgG3 than IgG2 and IgG4 [84], and the deposition extent of downstream complement mediators may vary by class as well [133]. The anti-BSA IgG used currently is polyclonal, consisting of a heterogenous mixture of IgG of various classes, and as such is subject to greater batch-to-batch variability. By utilizing a 'dummy' monoclonal activating IgG1 or IgG3, all originate from the same hybridoma clone and are therefore of the same class. A sought response could be more reliably engineered, although cost may be prohibitive. As complement-mediated damage to bystander cells is unavoidable given the nonspecific nature of the response, future work should select the complement-fixing IgG subclass that balances cytotoxicity with limited off-target effects. IgG spacing has also been shown to critically affect C1 complex avidity – IgG binding antigen on a surface may interact to form hexamers such that C1q may bind [26]. Thus far we have labeled the particles via passive adsorption, noting the highest complement activation and cytotoxicity without a preceding antigen layer [33]. However, this could be reevaluated in comparison to similar particles of a carboxyl density amenable to IgG spacing for hexamerization, with the antigen previously bound via EDC/NHS, for example. An approximate amount of IgG to add for this configuration could be estimated by attaining surface profiles via atomic force microscopy with varying extents of IgG coverage. MBL and ficolins (of the lectin pathway) may be useful, as well as engineered fusions of these [134].

IgG class selection may also affect the uptake of the particle-bound bacteria complex at the infection site. Upon binding anaphylatoxins released during the cascade (particularly C5a), neutrophils are attracted and bind the Fc region of IgG via the FcγRIIIb [84], and once additionally bound to opsonins (C3b, iC3b, C4b) via CR3 (complement receptor 3), initiate phagocytosis [135]. IgG1- and IgG3-labeled particles are taken up more effectively than those bound with IgG2 and IgG4, but the strongest preference is for IgG3 [136].

In addition to or instead of the selection of the most advantageous IgG class, changing particle chemical composition could also augment complement, as well as aim the platform toward clinical feasibility. Complement mediators may directly bind to chemical functionalities and initiate the alternative pathway, namely hydroxyl and carboxyl groups [42, 137]. Increasing carboxyl abundance was shown to also decrease avidity for Factor H binding, a component of the alternative pathway that catalyzes inactivation of surface-bound C3b [42]; C3b-spurred C5 convertase formation might continue longer, which would improve cytotoxicity. Our base particles are extensively carboxylated (~ 4/nm^2 [33]) and thus amenable to the alternative pathway, but are non-biodegradable, and at 1 μm may occlude finer capillaries. In addition, we have noted that smaller particles (.5 μm diameter) similarly conjugated with IgG activate the classical pathway more strongly [52]. However, there is likely a size cutoff where insufficient IgG to initiate complement is bound. Polymers or materials that degrade under normal or inflammatory physiological conditions will be utilized for further studies, particularly those that display a high number of functional groups (particularly nucleophilic groups such as amine [43, 138], hydroxyl [41, 138], and carboxyl [42] for C3b binding/derivatization. The polysaccharide chitosan could be suitable, as it is biodegradable *in vivo* to innocuous byproducts, its degradation time can be tuned by various factors controlled during its synthesis [139], it is heavily aminated

and carboxylated and can be further modified [140-142]. Further, chitosan possesses innate antibacterial properties – although not yet completely understood, high molecular weight chitosan may bind and destabilize components of the Gram-negative bacterial wall as it is strongly hydrophilic composition and negatively charged [143]. Lower molecular weight chitosan, though also antibacterial, tends to be less effective [144, 145]. Ma et al. demonstrated wide-range cytotoxicity against antibiotic resistant microbes with chitosan microparticles, which were unable to acquire resistance [146]. However, selectivity was not evaluated. Given that chitosan innately binds bacterial membranes and therefore complicates specificity in targeting, a chitosan coating of a degradable particle could be used as an adjuvant to spur complement with the coating Fc-conjugated to allow for targeting. Other materials of interest include carboxyl-terminated PEG-PLGA (poly(lactic-co-glycolic acid) and triblock-copolymer Pluronic F127 (polyethylene glycol – polypropylene glycol – polyethylene glycol). Both readily form micelles [147, 148]. Diblock carboxyl PEG-PLGA micelles form with the hydrophobic PLGA chains oriented inwards in aqueous environments, and carboxyl PEG chains oriented outwards [149]; a number of these carboxyl groups could be IgG-conjugated for targeting. The arrangement of the blocks can be modified to slow the hydrolysis of the ester linkages in the PLGA, extending circulation time [150]. Given that PEG characteristically inhibits opsonization, intermolecular spacing between PEG molecules on the particle surface as well as their surface density must be carefully analyzed given the synthesis conditions to preserve complement activation [151]. Should smaller particles be utilized to improve complement response, bare carboxyl-terminated PLGA might be more suitable to better prevent cell uptake [150]. Carboxyl-terminated Pluronic F127 can allow for derivatization of constituent micelles with peptides and other thiol-containing biomolecules via pyridyl disulfide modification [152]. The polypropylene glycol core block

degrades with exposure to oxidizing species [42, 152], such as those released during respiratory burst of neutrophils or macrophages. There is also evidence that amplification of the alternative pathway is also facilitated by infiltrating neutrophils in a positive feedback loop mediated by neutrophil deposition of properdin upon bystander cells [153]. To further stimulate neutrophils, slowly-degrading micelles of carboxyl-PEG-PLGA or carboxyl-terminated Pluronic F127 could encapsulate hydrophobic immunostimulatory molecules such as the potent neutrophil chemoattractant peptide N-Formylmethionyl-leucyl-phenylalanine (fMLP) and/or superoxide inducer phorbol myristate acetate (PMA) [153]. To avoid severe complications, this would be contraindicated for sepsis. Morphological modifications can also be made to improve neutrophil uptake; particles with extensive microtexture can speed neutrophil recruitment and uptake in addition to increasing inflammasome activation [154].

REFERENCES

1. Magiorakos, A.P., et al., *Multidrug-resistant, extensively drug-resistant and pandrug-resistant bacteria: an international expert proposal for interim standard definitions for acquired resistance.* Clinical Microbiology and Infection. **18**(3): p. 268-281.
2. Watkins, R.R. and R.A. Bonomo, *Overview: Global and Local Impact of Antibiotic Resistance.* Infect Dis Clin North Am, 2016. **30**(2): p. 313-22.
3. CDC, *Antibiotic Resistance Threats in the United States* 2013.
4. Katz, M.L., et al., *Where have all the antibiotic patents gone?* Nat Biotech, 2006. **24**(12): p. 1529-1531.
5. WHO, *Antimicrobial Resistance: Global Report on Surveillance 2014.* 2014.
6. Shlaes, D.M., et al., *The FDA Reboot of Antibiotic Development.* Antimicrobial Agents and Chemotherapy, 2013. **57**(10): p. 4605-4607.
7. Lushniak, B.D., *Antibiotic resistance: a public health crisis.* Public Health Rep, 2014. **129**(4): p. 314-6.
8. Gould, I.M. and A.M. Bal, *New antibiotic agents in the pipeline and how they can help overcome microbial resistance.* Virulence, 2013. **4**(2): p. 185-191.
9. J., O.N., *Review on Antimicrobial Resistance Antimicrobial Resistance: Tackling a Crisis for the Health and Wealth of Nations.* . London: Review on Antimicrobial Resistance, 2014.
10. Yoon, M.Y., K. Lee, and S.S. Yoon, *Protective role of gut commensal microbes against intestinal infections.* Journal of Microbiology, 2014. **52**(12): p. 983-989.
11. Tlaskalova-Hogenova, H., et al., *The role of gut microbiota (commensal bacteria) and the mucosal barrier in the pathogenesis of inflammatory and autoimmune diseases and cancer: contribution of germ-free and gnotobiotic animal models of human diseases.* Cell Mol Immunol, 2011. **8**(2): p. 110-120.
12. Zipperer, A., et al., *Human commensals producing a novel antibiotic impair pathogen colonization.* Nature, 2016. **535**(7613): p. 511-6.
13. Knoop, K.A., et al., *Antibiotics promote inflammation through the translocation of native commensal colonic bacteria.* Gut, 2016. **65**(7): p. 1100-9.
14. Hviid, A., H. Svanström, and M. Frisch, *Antibiotic use and inflammatory bowel diseases in childhood.* Gut, 2011. **60**(1): p. 49-54.
15. Candon, S., et al., *Antibiotics in Early Life Alter the Gut Microbiome and Increase Disease Incidence in a Spontaneous Mouse Model of Autoimmune Insulin-Dependent Diabetes.* PLOS ONE, 2015. **10**(5): p. e0125448.
16. Wen, L., et al., *Innate immunity and intestinal microbiota in the development of Type 1 diabetes.* Nature, 2008. **455**(7216): p. 1109-1113.
17. Merle NS, C.S., Fremeaux-Bacchi V, Roumenina LT, *Complement System Part I - Molecular Mechanisms of Activation and Regulation.* Front Immunol., 2015. **6**.
18. Ricklin D, H.G., Yang K, Lambris JD., *Complement: a key system for immune surveillance and homeostasis.* Nat Immunol. , 2010. **11**(9): p. 785-97.
19. Sjöberg AP, T.L., Blom AM, *Complement activation and inhibition: a delicate balance.* Trends Immunol. , 2009. **30**(2): p. 83-90.
20. Arvieux, J., H. Yssel, and M.G. Colomb, *Antigen-bound C3b and C4b enhance antigen-presenting cell function in activation of human T-cell clones.* Immunology, 1988. **65**(2): p. 229-235.

21. Merle NS, N.R., Halbwachs-Mecarelli L, Fremeaux-Bacchi V, Roumenina LT., *Complement System Part II: Role in Immunity.* Front Immunol., 2015. **6**.
22. Reddy, S.T., et al., *Exploiting lymphatic transport and complement activation in nanoparticle vaccines.* Nature biotechnology, 2007. **25**(10): p. 1159-1164.
23. Moghimi, S.M., et al., *Material properties in complement activation.* Advanced drug delivery reviews, 2011. **63**(12): p. 1000-7.
24. Montdargent, B., D. Labarre, and M. Jozefowicz, *Interactions of functionalized polystyrene derivatives with the complement system in human serum.* Journal of biomaterials science. Polymer edition, 1991. **2**(1): p. 25-35.
25. Szebeni, J., et al., *Activation of complement by therapeutic liposomes and other lipid excipient-based therapeutic products: prediction and prevention.* Advanced drug delivery reviews, 2011. **63**(12): p. 1020-30.
26. Diebolder, C.A., et al., *Complement Is Activated by IgG Hexamers Assembled at the Cell Surface.* Science, 2014. **343**(6176): p. 1260-1263.
27. Burton, D.R., *Is IgM-like dislocation a common feature of antibody function?* Immunology Today, 1986. **7**(6): p. 165-167.
28. Berends, E.T.M., et al., *Bacteria under stress by complement and coagulation.* FEMS Microbiology Reviews, 2014. **38**(6): p. 1146-1171.
29. Tan, L.A., et al., *Interactions of complement proteins C1q and factor H with lipid A and Escherichia coli: further evidence that factor H regulates the classical complement pathway.* Protein Cell, 2011. **2**(4): p. 320-32.
30. Paidassi, H., et al., *The lectin-like activity of human C1q and its implication in DNA and apoptotic cell recognition.* FEBS Lett, 2008. **582**(20): p. 3111-6.
31. Janeway CA Jr, Travers P, and Walport M, *Immunobiology: The Immune System in Health and Disease.* The complement system and innate immunity. 2001, New York: Garland Science.
32. Shin, H.S., et al., *Chemotactic and Anaphylatoxic Fragment Cleaved from the Fifth Component of Guinea Pig Complement.* Science, 1968. **162**(3851): p. 361-363.
33. Holt BA, B.M., Potter D, White D, Stowell SR, Sulchek T, *Fc microparticles can modulate the physical extent and magnitude of complement activity.* Biomater Sci., 2017. **5**(3): p. 463-474.
34. Ali, Y.M., et al., *The Lectin Pathway of Complement Activation Is a Critical Component of the Innate Immune Response to Pneumococcal Infection.* PLOS Pathogens, 2012. **8**(7): p. e1002793.
35. Carlsson, M., et al., *Deficiency of the mannan-binding lectin pathway of complement and poor outcome in cystic fibrosis: bacterial colonization may be decisive for a relationship.* Clinical and Experimental Immunology, 2005. **139**(2): p. 306-313.
36. Vonarbourg, A., et al., *Parameters influencing the stealthiness of colloidal drug delivery systems.* Biomaterials, 2006. **27**(24): p. 4356-73.
37. Jiang, S. and Z. Cao, *Ultralow-fouling, functionalizable, and hydrolyzable zwitterionic materials and their derivatives for biological applications.* Adv Mater, 2010. **22**(9): p. 920-32.
38. Kopf, M., et al., *Complement component C3 promotes T-cell priming and lung migration to control acute influenza virus infection.* Nat Med, 2002. **8**(4): p. 373-8.

39. Schmidt, J., et al., *Release of iC3b from apoptotic tumor cells induces tolerance by binding to immature dendritic cells in vitro and in vivo.* Cancer Immunology, Immunotherapy, 2006. **55**(1): p. 31-38.
40. Sohn, J.-H., et al., *Tolerance is dependent on complement C3 fragment iC3b binding to antigen-presenting cells.* Nat Med, 2003. **9**(2): p. 206-212.
41. Reddy, S.T., et al., *Exploiting lymphatic transport and complement activation in nanoparticle vaccines.* Nature Biotechnology, 2007. **25**(10): p. 1159-1164.
42. Thomas, S.N., et al., *Engineering complement activation on polypropylene sulfide vaccine nanoparticles.* Biomaterials, 2011. **32**(8): p. 2194-203.
43. Liu, Y., et al., *Engineering biomaterial-associated complement activation to improve vaccine efficacy.* Biomacromolecules, 2013. **14**(9): p. 3321-8.
44. Mueller, S.N., S. Tian, and J.M. DeSimone, *Rapid and Persistent Delivery of Antigen by Lymph Node Targeting PRINT Nanoparticle Vaccine Carrier To Promote Humoral Immunity.* Molecular Pharmaceutics, 2015. **12**(5): p. 1356-1365.
45. Diebolder, C.A., et al., *Complement Is Activated by IgG Hexamers Assembled at the Cell Surface.* Science (New York, N.Y.), 2014. **343**(6176): p. 1260-1263.
46. Hughes-Jones, N.C., et al., *Antibody density on rat red cells determines the rate of activation of the complement component C1.* Eur J Immunol, 1985. **15**(10): p. 976-80.
47. Cragg, M.S., et al., *Complement-mediated lysis by anti-CD20 mAb correlates with segregation into lipid rafts.* Blood, 2003. **101**(3): p. 1045-52.
48. Ahsan, F., et al., *Targeting to macrophages: role of physicochemical properties of particulate carriers--liposomes and microspheres--on the phagocytosis by macrophages.* J Control Release, 2002. **79**(1-3): p. 29-40.
49. Gallo, P., R. Gonçalves, and D.M. Mosser, *The influence of IgG Density and Macrophage Fc (gamma) Receptor Cross-linking on Phagocytosis and IL-10 Production.* Immunology letters, 2010. **133**(2): p. 70-77.
50. Pacheco, P., D. White, and T. Sulchek, *Effects of Microparticle Size and Fc Density on Macrophage Phagocytosis.* PLoS One, 2013. **8**(4).
51. Champion, J.A., A. Walker, and S. Mitragotri, *Role of particle size in phagocytosis of polymeric microspheres.* Pharm Res, 2008. **25**(8): p. 1815-21.
52. Pacheco, P., et al., *Tunable Complement Activation by Particles with Variable Size and Fc Density.* Nano LIFE, 2013. **3**.
53. Ma, Y.G., et al., *Human mannose-binding lectin and L-ficolin function as specific pattern recognition proteins in the lectin activation pathway of complement.* J Biol Chem, 2004. **279**(24): p. 25307-12.
54. Jack, D.L. and M.W. Turner, *Anti-microbial activities of mannose-binding lectin.* Biochem Soc Trans, 2003. **31**(Pt 4): p. 753-7.
55. Nadesalingam, J., et al., *Mannose-binding lectin recognizes peptidoglycan via the N-acetyl glucosamine moiety, and inhibits ligand-induced proinflammatory effect and promotes chemokine production by macrophages.* J Immunol, 2005. **175**(3): p. 1785-94.
56. Du Clos, T.W., *Pentraxins: structure, function, and role in inflammation.* ISRN Inflamm, 2013. **2013**: p. 379040.
57. Merino, S., et al., *Activation of the Complement Classical Pathway (C1q Binding) by Mesophilic Aeromonas hydrophila Outer Membrane Protein.* Infection and Immunity, 1998. **66**(8): p. 3825-3831.

58. Spitzer, D., et al., *Properdin can initiate complement activation by binding specific target surfaces and providing a platform for de novo convertase assembly.* J Immunol, 2007. **179**(4): p. 2600-8.
59. Tommasi, R., et al., *ESKAPEing the labyrinth of antibacterial discovery.* Nat Rev Drug Discov, 2015. **14**(8): p. 529-42.
60. Lukjancenko, O., T.M. Wassenaar, and D.W. Ussery, *Comparison of 61 Sequenced Escherichia coli Genomes.* Microbial Ecology, 2010. **60**(4): p. 708-720.
61. Orskov, I., et al., *Serology, chemistry, and genetics of O and K antigens of Escherichia coli.* Bacteriological Reviews, 1977. **41**(3): p. 667-710.
62. Mollnes, T.E., et al., *Essential role of the C5a receptor in E coli-induced oxidative burst and phagocytosis revealed by a novel lepirudin-based human whole blood model of inflammation.* Blood, 2002. **100**(5): p. 1869-77.
63. Doorduijn, D.J., et al., *Complement resistance mechanisms of Klebsiella pneumoniae.* Immunobiology, 2016. **221**(10): p. 1102-1109.
64. Riley , L.W., et al., *Hemorrhagic Colitis Associated with a Rare Escherichia coli Serotype.* New England Journal of Medicine, 1983. **308**(12): p. 681-685.
65. Lim, J.Y., J.W. Yoon, and C.J. Hovde, *A Brief Overview of Escherichia coli O157:H7 and Its Plasmid O157.* Journal of microbiology and biotechnology, 2010. **20**(1): p. 5-14.
66. Banatvala, N., et al., *The United States National Prospective Hemolytic Uremic Syndrome Study: microbiologic, serologic, clinical, and epidemiologic findings.* J Infect Dis, 2001. **183**(7): p. 1063-70.
67. Proulx, F., E.G. Seidman, and D. Karpman, *Pathogenesis of Shiga Toxin-Associated Hemolytic Uremic Syndrome.* Pediatr Res, 2001. **50**(2): p. 163-171.
68. Johannes, L. and W. Romer, *Shiga toxins [mdash] from cell biology to biomedical applications.* Nat Rev Micro, 2010. **8**(2): p. 105-116.
69. Obrig, T.G., T.P. Moran, and J.E. Brown, *The mode of action of Shiga toxin on peptide elongation of eukaryotic protein synthesis.* Biochem J, 1987. **244**(2): p. 287-94.
70. Grif, K., et al., *Strain-specific differences in the amount of Shiga toxin released from enterohemorrhagic Escherichia coli O157 following exposure to subinhibitory concentrations of antimicrobial agents.* Eur J Clin Microbiol Infect Dis, 1998. **17**(11): p. 761-6.
71. Wong , C.S., et al., *The Risk of the Hemolytic–Uremic Syndrome after Antibiotic Treatment of Escherichia coli O157:H7 Infections.* New England Journal of Medicine, 2000. **342**(26): p. 1930-1936.
72. Noris, M., F. Mescia, and G. Remuzzi, *STEC-HUS, atypical HUS and TTP are all diseases of complement activation.* Nat Rev Nephrol, 2012. **8**(11): p. 622-633.
73. Ståhl, A.-l., L. Sartz, and D. Karpman, *Complement activation on platelet-leukocyte complexes and microparticles in enterohemorrhagic Escherichia coli–induced hemolytic uremic syndrome.* Blood, 2011. **117**(20): p. 5503-5513.
74. Conway, E.M., *HUS and the case for complement.* Blood, 2015. **126**(18): p. 2085-90.
75. Arvidsson, I., et al., *Early Terminal Complement Blockade and C6 Deficiency Are Protective in Enterohemorrhagic Escherichia coli–Infected Mice.* The Journal of Immunology, 2016.
76. Orth, D., et al., *EspP, a serine protease of enterohemorrhagic Escherichia coli, impairs complement activation by cleaving complement factors C3/C3b and C5.* Infect Immun, 2010. **78**(10): p. 4294-301.

77. Miner, K.M., et al., *Characterization of murine monoclonal antibodies to Escherichia coli J5.* Infect Immun, 1986. **52**(1): p. 56-62.
78. Braude, A.I. and H. Douglas, *Passive immunization against the local Shwartzman reaction.* J Immunol, 1972. **108**(2): p. 505-12.
79. Braude, A.I., H. Douglas, and C.E. Davis, *Treatment and prevention of intravascular coagulation with antiserum to endotoxin.* J Infect Dis, 1973. **128**: p. Suppl:157-64.
80. Ziegler, E.J., et al., *Prevention of lethal pseudomonas bacteremia with epimerase-deficient E. coli antiserum.* Trans Assoc Am Physicians, 1975. **88**: p. 101-8.
81. Hermanson, G.T., *Chapter 4 - Zero-Length Crosslinkers*, in *Bioconjugate Techniques (Third edition)*. 2013, Academic Press: Boston. p. 259-273.
82. Neogi, P., *Inhomogeneity of adsorbed proteins on a solid surface.* Colloids Surf B Biointerfaces, 2009. **71**(1): p. 119-23.
83. Lundqvist, M., et al., *Nanoparticle size and surface properties determine the protein corona with possible implications for biological impacts.* Proc Natl Acad Sci U S A, 2008. **105**(38): p. 14265-70.
84. Vidarsson, G., G. Dekkers, and T. Rispens, *IgG Subclasses and Allotypes: From Structure to Effector Functions.* Frontiers in Immunology, 2014. **5**: p. 520.
85. Lundqvist, M., et al., *Nanoparticle size and surface properties determine the protein corona with possible implications for biological impacts.* Proceedings of the National Academy of Sciences, 2008. **105**(38): p. 14265-14270.
86. Samant, S., et al., *Nucleotide Biosynthesis Is Critical for Growth of Bacteria in Human Blood.* PLoS Pathogens, 2008. **4**(2): p. e37.
87. TOMASIEWICZ, D.M., et al., *The Most Suitable Number of Colonies on Plates for Counting.* Journal of Food Protection, 1980. **43**(4): p. 282-286.
88. Breed, R.S. and W.D. Dotterrer, *The Number of Colonies Allowable on Satisfactory Agar Plates.* J Bacteriol, 1916. **1**(3): p. 321-31.
89. Sutton, S., *Accuracy of Plate Counts.* Journal of Validation Technology, 2011. **17**(3): p. 42-46.
90. Onoda, T., et al., *Effects of calcium and calcium chelators on growth and morphology of Escherichia coli L-form NC-7.* J Bacteriol, 2000. **182**(5): p. 1419-22.
91. Hong, Y.Q. and B. Ghebrehiwet, *Effect of Pseudomonas aeruginosa elastase and alkaline protease on serum complement and isolated components C1q and C3.* Clin Immunol Immunopathol, 1992. **62**(2): p. 133-8.
92. Miajlovic, H. and S.G. Smith, *Bacterial self-defence: how Escherichia coli evades serum killing.* FEMS Microbiol Lett, 2014. **354**(1): p. 1-9.
93. Lambris, J.D., D. Ricklin, and B.V. Geisbrecht, *Complement evasion by human pathogens.* Nat Rev Microbiol, 2008. **6**(2): p. 132-42.
94. Archer, N.K., et al., *Staphylococcus aureus biofilms: Properties, regulation and roles in human disease.* Virulence, 2011. **2**(5): p. 445-459.
95. Neil, R.B. and M.A. Apicella, *Clinical and laboratory evidence for Neisseria meningitidis biofilms.* Future microbiology, 2009. **4**: p. 555-563.
96. Donlan, R.M., *Biofilms: Microbial Life on Surfaces.* Emerging Infectious Diseases, 2002. **8**(9): p. 881-890.
97. Morrison, D.C. and D.M. Jacobs, *Binding of polymyxin B to the lipid A portion of bacterial lipopolysaccharides.* Immunochemistry, 1976. **13**(10): p. 813-818.

98. Hogasen, A.K. and T.G. Abrahamsen, *Polymyxin B stimulates production of complement components and cytokines in human monocytes.* Antimicrob Agents Chemother, 1995. **39**(2): p. 529-32.
99. Gordon, D.L., J.L. Rice, and P.J. McDonald, *Regulation of human neutrophil type 3 complement receptor (iC3b receptor) expression during phagocytosis of Staphylococcus aureus and Escherichia coli.* Immunology, 1989. **67**(4): p. 460-465.
100. Rose, F., et al., *Targeting lipopolysaccharides by the nontoxic polymyxin B nonapeptide sensitizes resistant Escherichia coli to the bactericidal effect of human neutrophils.* J Infect Dis, 2000. **182**(1): p. 191-9.
101. Vaara, M. and T. Vaara, *Sensitization of Gram-negative bacteria to antibiotics and complement by a nontoxic oligopeptide.* Nature, 1983. **303**(5917): p. 526-8.
102. Nakae, H., et al., *Serum complement levels and severity of sepsis.* Res Commun Chem Pathol Pharmacol, 1994. **84**(2): p. 189-95.
103. Bogdanovich, T., et al., *Colistin-resistant, Klebsiella pneumoniae carbapenemase (KPC)-producing Klebsiella pneumoniae belonging to the international epidemic clone ST258.* Clin Infect Dis, 2011. **53**(4): p. 373-6.
104. Mansour, W., et al., *Outbreak of colistin-resistant carbapenemase-producing Klebsiella pneumoniae in Tunisia.* Journal of Global Antimicrobial Resistance, 2017. **10**(Supplement C): p. 88-94.
105. Liu, Y.Y., et al., *Emergence of plasmid-mediated colistin resistance mechanism MCR-1 in animals and human beings in China: a microbiological and molecular biological study.* Lancet Infect Dis, 2016. **16**(2): p. 161-8.
106. Schwarz, S. and A.P. Johnson, *Transferable resistance to colistin: a new but old threat.* Journal of Antimicrobial Chemotherapy, 2016. **71**(8): p. 2066-2070.
107. Markiewski, M.M., R.A. DeAngelis, and J.D. Lambris, *Complexity of complement activation in sepsis.* Journal of Cellular and Molecular Medicine, 2008. **12**(6a): p. 2245-2254.
108. de Breij, A., et al., *The antimicrobial peptide SAAP-148 combats drug-resistant bacteria and biofilms.* Science Translational Medicine, 2018. **10**(423).
109. Hou, M., et al., *Antimicrobial peptide LL-37 and IDR-1 ameliorate MRSA pneumonia in vivo.* Cell Physiol Biochem, 2013. **32**(3): p. 614-23.
110. Hancock, R.E. and A. Rozek, *Role of membranes in the activities of antimicrobial cationic peptides.* FEMS Microbiol Lett, 2002. **206**(2): p. 143-9.
111. Luo, Y., et al., *The Naturally Occurring Host Defense Peptide, LL-37, and Its Truncated Mimetics KE-18 and KR-12 Have Selected Biocidal and Antibiofilm Activities Against Candida albicans, Staphylococcus aureus, and Escherichia coli In vitro.* Frontiers in Microbiology, 2017. **8**: p. 544.
112. Singh, D., et al., *The Human Antimicrobial Peptide LL-37, but Not the Mouse Ortholog, mCRAMP, Can Stimulate Signaling by Poly(I:C) through a FPRL1-dependent Pathway.* The Journal of Biological Chemistry, 2013. **288**(12): p. 8258-8268.
113. Ciornei, C.D., et al., *Antimicrobial and chemoattractant activity, lipopolysaccharide neutralization, cytotoxicity, and inhibition by serum of analogs of human cathelicidin LL-37.* Antimicrob Agents Chemother, 2005. **49**(7): p. 2845-50.
114. Mahon, J.L. and C.R. Stiller, *The Immunocompromised Patient.* Canadian Family Physician, 1987. **33**: p. 349-359.

115. Bassetti, M., et al., *Epidemiological trends in nosocomial candidemia in intensive care.* BMC Infectious Diseases, 2006. **6**(1): p. 21.
116. Morgan, J., et al., *Excess mortality, hospital stay, and cost due to candidemia: a case-control study using data from population-based candidemia surveillance.* Infect Control Hosp Epidemiol, 2005. **26**(6): p. 540-7.
117. Berkow, E.L. and S.R. Lockhart, *Fluconazole resistance in Candida species: a current perspective.* Infection and Drug Resistance, 2017. **10**: p. 237-245.
118. Vallabhaneni, S., et al., *Epidemiology and Risk Factors for Echinocandin Nonsusceptible Candida glabrata Bloodstream Infections: Data From a Large Multisite Population-Based Candidemia Surveillance Program, 2008–2014.* Open Forum Infectious Diseases, 2015. **2**(4): p. ofv163.
119. Laniado-Laborin, R. and M.N. Cabrales-Vargas, *Amphotericin B: side effects and toxicity.* Rev Iberoam Micol, 2009. **26**(4): p. 223-7.
120. Spellberg, B., *Novel Insights into Disseminated Candidiasis: Pathogenesis Research and Clinical Experience Converge.* PLoS Pathogens, 2008. **4**(2): p. e38.
121. Kozel, T.R., *Activation of the complement system by pathogenic fungi.* Clin Microbiol Rev, 1996. **9**(1): p. 34-46.
122. Johnson, N., *The role of natural antibodies in complement activation by non-albicans Candida species.* Unpublished Master's Thesis, 2011.
123. Marcos, C.M., et al., *Anti-Immune Strategies of Pathogenic Fungi.* Frontiers in Cellular and Infection Microbiology, 2016. **6**: p. 142.
124. Meri, T., et al., *The Yeast Candida albicans Binds Complement Regulators Factor H and FHL-1.* Infection and Immunity, 2002. **70**(9): p. 5185-5192.
125. Tsoni, S.V., et al., *Complement C3 Plays an Essential Role in the Control of Opportunistic Fungal Infections.* Infection and Immunity, 2009. **77**(9): p. 3679-3685.
126. Ashman, R.B., et al., *Role of complement C5 and T lymphocytes in pathogenesis of disseminated and mucosal candidiasis in susceptible DBA/2 mice.* Microb Pathog, 2003. **34**(2): p. 103-13.
127. Adams, E.K., D.S. Ashcraft, and G.A. Pankey, *In vitro Synergistic Activity of Caspofungin Plus Polymyxin B Against Fluconazole-Resistant Candida glabrata.* Am J Med Sci, 2016. **351**(3): p. 265-70.
128. Pietschmann, S., et al., *Synergistic effects of Miconazole and Polymyxin B on microbial pathogens.* Veterinary Research Communications, 2009. **33**(6): p. 489-505.
129. Zhai, B., et al., *Polymyxin B, in combination with fluconazole, exerts a potent fungicidal effect.* Journal of Antimicrobial Chemotherapy, 2010. **65**(5): p. 931-938.
130. Boxx, G.M., et al., *Influence of Mannan and Glucan on Complement Activation and C3 Binding by Candida albicans.* Infection and Immunity, 2010. **78**(3): p. 1250-1259.
131. Fitzpatrick, D.A., M.E. Logue, and G. Butler, *Evidence of recent interkingdom horizontal gene transfer between bacteria and Candida parapsilosis.* BMC Evolutionary Biology, 2008. **8**(1): p. 181.
132. Gressner, O.A., et al., *High C5a levels are associated with increased mortality in sepsis patients--no enhancing effect by actin-free Gc-globulin.* Clin Biochem, 2008. **41**(12): p. 974-80.
133. Bindon, C.I., et al., *Human monoclonal IgG isotypes differ in complement activating function at the level of C4 as well as C1q.* J Exp Med, 1988. **168**(1): p. 127-42.

134. Michelow, I.C., et al., *A Novel L-ficolin/Mannose-binding Lectin Chimeric Molecule with Enhanced Activity against Ebola Virus.* The Journal of Biological Chemistry, 2010. **285**(32): p. 24729-24739.
135. Le Cabec, V., et al., *Complement receptor 3 (CD11b/CD18) mediates type I and type II phagocytosis during nonopsonic and opsonic phagocytosis, respectively.* J Immunol, 2002. **169**(4): p. 2003-9.
136. Bruhns, P., et al., *Specificity and affinity of human Fcgamma receptors and their polymorphic variants for human IgG subclasses.* Blood, 2009. **113**(16): p. 3716-25.
137. Arima, Y., et al., *Complement Activation by Polymers Carrying Hydroxyl Groups.* ACS Applied Materials & Interfaces, 2009. **1**(10): p. 2400-2407.
138. Law, S.K. and A.W. Dodds, *The internal thioester and the covalent binding properties of the complement proteins C3 and C4.* Protein Sci, 1997. **6**(2): p. 263-74.
139. Szymańska, E. and K. Winnicka, *Stability of Chitosan—A Challenge for Pharmaceutical and Biomedical Applications.* Marine Drugs, 2015. **13**(4): p. 1819-1846.
140. Lillo, L.E. and B. Matsuhiro, *Chemical modifications of carboxylated chitosan.* Carbohydrate Polymers, 1997. **34**(4): p. 397-401.
141. Buzzacchera, I., et al., *Polymer Brush-Functionalized Chitosan Hydrogels as Antifouling Implant Coatings.* Biomacromolecules, 2017. **18**(6): p. 1983-1992.
142. Hou, J., et al., *Triphenyl Phosphine-Functionalized Chitosan Nanoparticles Enhanced Antitumor Efficiency Through Targeted Delivery of Doxorubicin to Mitochondria.* Nanoscale Research Letters, 2017. **12**(1): p. 158.
143. Muzzarelli, R., et al., *Antimicrobial properties of N-carboxybutyl chitosan.* Antimicrob Agents Chemother, 1990. **34**(10): p. 2019-23.
144. Shin, Y., D.I. Yoo, and J. Jang, *Molecular weight effect on antimicrobial activity of chitosan treated cotton fabrics.* Journal of Applied Polymer Science, 2001. **80**(13): p. 2495-2501.
145. Li, J., Y. Wu, and L. Zhao, *Antibacterial activity and mechanism of chitosan with ultra high molecular weight.* Carbohydrate Polymers, 2016. **148**(Supplement C): p. 200-205.
146. Ma, Z., et al., *Chitosan Microparticles Exert Broad-Spectrum Antimicrobial Activity against Antibiotic-Resistant Micro-organisms without Increasing Resistance.* ACS Appl Mater Interfaces, 2016. **8**(17): p. 10700-9.
147. Ashjari, M., et al., *Self-assembled nanomicelles using PLGA-PEG amphiphilic block copolymer for insulin delivery: a physicochemical investigation and determination of CMC values.* J Mater Sci Mater Med, 2012. **23**(4): p. 943-53.
148. Basak, R. and R. Bandyopadhyay, *Encapsulation of Hydrophobic Drugs in Pluronic F127 Micelles: Effects of Drug Hydrophobicity, Solution Temperature, and pH.* Langmuir, 2013. **29**(13): p. 4350-4356.
149. Makadia, H.K. and S.J. Siegel, *Poly Lactic-co-Glycolic Acid (PLGA) as Biodegradable Controlled Drug Delivery Carrier.* Polymers, 2011. **3**(3): p. 1377-1397.
150. Sah, H., et al., *Concepts and practices used to develop functional PLGA-based nanoparticulate systems.* International Journal of Nanomedicine, 2013. **8**: p. 747-765.
151. Vittaz, M., et al., *Effect of PEO surface density on long-circulating PLA-PEO nanoparticles which are very low complement activators.* Biomaterials, 1996. **17**(16): p. 1575-1581.

152. van der Vlies, A.J., et al., *Synthesis of Pyridyl Disulfide-Functionalized Nanoparticles for Conjugating Thiol-Containing Small Molecules, Peptides, and Proteins.* Bioconjugate Chemistry, 2010. **21**(4): p. 653-662.
153. Camous, L., et al., *Complement alternative pathway acts as a positive feedback amplification of neutrophil activation.* Blood, 2011. **117**(4): p. 1340-1349.
154. Vaine, C.A., et al., *Tuning innate immune activation by surface texturing of polymer microparticles: the role of shape in inflammasome activation().* Journal of immunology (Baltimore, Md. : 1950), 2013. **190**(7): p. 3525-3532.